

PRESSIO: ENABLING PROJECTION-BASED MODEL REDUCTION FOR LARGE-SCALE NONLINEAR DYNAMICAL SYSTEMS *

FRANCESCO RIZZI[†], PATRICK J. BLONIGAN[‡], ERIC J. PARISH[‡], AND
KEVIN T. CARLBERG^{‡§}

Abstract. This work introduces **Pressio**, an open-source project aimed at enabling leading-edge projection-based reduced order models (ROMs) for large-scale nonlinear dynamical systems in science and engineering. **Pressio** provides model-reduction methods that can reduce both the number of spatial and temporal degrees of freedom for any dynamical system expressible as a system of parameterized ordinary differential equations (ODEs). We leverage this simple, expressive mathematical framework as a pivotal design choice to enable a minimal application programming interface (API) that is natural to dynamical systems. The core component of **Pressio** is a C++11 header-only library that leverages generic programming to support applications with arbitrary data types and arbitrarily complex programming models. This is complemented with Python bindings to expose these C++ functionalities to Python users with negligible overhead and no user-required binding code. We discuss the distinguishing characteristics of **Pressio** relative to existing model-reduction libraries, outline its key design features, describe how the user interacts with it, and present two test cases—including one with over 20 million degrees of freedom—that highlight the performance results of **Pressio** and illustrate the breath of problems that can be addressed with it.

Key words. projection-based model reduction, Galerkin, LSPG, POD, SVD, sample mesh, hyper-reduction, scientific computing, object-oriented programming, generic programming, policy-based design, design by introspection, template metaprogramming, HPC, Kokkos, Trilinos, Python.

AMS subject classifications. 65L05, 65L06, 65M12, 68U20, 68N15, 68W10, 68W15, 68N01, 76K05

1. Introduction. Computational science and engineering has become a fundamental driver of the technological advancement of modern society, underpinning applications such as scientific discovery, engineering design, vehicle control, infrastructure monitoring, and risk assessment of engineered systems. Computational science and engineering and high-performance computing have a symbiotic relationship: the constant improvement and availability of computing power drives the ambition to model increasingly complex systems with increasing levels of fidelity, which, in turn, motivates the pursuit of more powerful computing platforms.

The present “extreme-scale” computing era—often referred to as the dawn of exascale computing—is one of unprecedented access to computational resources. In principle, this enables scientists and engineers to tackle very complex problems that are *time critical* or *many query* in nature. Time-critical problems are those constrained by a limited wall-clock time, and include fast-turnaround design, rapid path planning, and model predictive control, which require simulations to execute on the order of hours, minutes, or milliseconds, respectively. In contrast, many-query problems are characterized by a limited budget of computational core-hours. Many-query problems pervade uncertainty quantification (UQ), as such applications typically require thousands of model evaluations to characterize adequately the effect of uncertainties in parameters and operating conditions on the system response. In the case of both

*Submitted to the editors February 6th, 2020.

[†]NexGen Analytics, 30N Gould St. Ste 5912, Sheridan, WY, 82801, USA (francesco.rizzi@ng-analytics.com, fnrizzi@sandia.gov).

[‡]Department of Extreme-Scale Data Science and Analytics, Sandia National Laboratories, Livermore, CA, 94550, USA (pblonig@sandia.gov, ejparis@sandia.gov).

[§]Departments of Applied Mathematics and Mechanical Engineering, University of Washington, Seattle, WA 98195, USA

time-critical and many-query problems, if the system of interest is computationally expensive to query—as in the case of high-fidelity models for which a single run can consume days or weeks on a supercomputer—the constraint on wall-clock time or core-hours can be impossible to satisfy. In such scenarios, analysts often turn to surrogate models, which replace the high-fidelity model with a lower-cost, lower-fidelity counterpart that can be employed within the application to make satisfaction of the wall-clock-time or core-hour constraint feasible. In this work, we consider the high-fidelity model of interest to be a nonlinear dynamical system expressible as a system of parameterized ordinary differential equations (ODEs).

Broadly speaking, surrogate models can be classified under three categories, namely (a) *data fits*, which construct an explicit mapping (e.g., using polynomials, Gaussian processes) from the system’s parameters (i.e., inputs) to the system response of interest (i.e., outputs), (b) *lower-fidelity models*, which simplify the high-fidelity model (e.g., by coarsening the mesh, employing a lower finite-element order, or neglecting physics), and (c) *projection-based reduced-order models (ROMs)*, which reduce the number of degrees of freedom in the high-fidelity model through a projection process. In general, data fits and lower-fidelity models are widely considered much easier to implement than ROMs, as they generally do not require any modifications to the underlying simulation code; however, because ROMs apply a projection process directly to the equations governing the high-fidelity model, one can often make much stronger performance guarantees (e.g., of structure preservation, of accuracy via adaptivity) and perform more accurate *a posteriori* error analysis (e.g., via *a posteriori* error bounds or error models) with ROMs. Despite these benefits, the practical challenges of implementing nonlinear model-reduction techniques in large-scale codes often precludes their adoption in practice; this occurs because naïve implementations require modifying low-level operations and solvers for each simulation code of interest. This implementation strategy is simply not practical or sustainable in many modern settings, because industrial simulation codes often evolve rapidly, institutions may employ dozens of simulation codes for different analyses, and commercial codes typically do not expose the required low-level operators and solvers. This challenge poses perhaps the single largest barrier to widespread adoption of model reduction in industrial applications.

To this end, this paper presents an open-source project that aims to mitigate the implementation burden of nonlinear model reduction in large-scale applications without compromising performance. We organize the introduction by first discussing existing packages for ROMs, some of their limitations, and then describe in detail what we propose.

Overview of the current software landscape. As previously mentioned, from a software standpoint, most approaches developed so far for ROMs have relied on intrusive implementations into each code of interest, see, e.g., the work in [25, 26, 17, 20, ?, ?, ?, ?]. This is impractical for two main reasons: first, each existing method needs to be re-implemented in any application adapting to various data structure and model; second, any time a new ROM algorithm is designed, it would require a separate implementation within each individual code. To overcome this barrier, recent works such as **modred** [5], **libROM**¹, **pyMOR** [30], and **pyROM** [33] have sought to provide frameworks for projection-based ROMs and related capabilities that can be used by external codes without requiring them to add model-reduction-specific code.

¹<https://github.com/LLNL/libROM>

libROM is a C++ library mainly focused on providing functionalities to compute proper orthogonal decomposition (POD) basis vectors from a matrix of samples state vectors. The key feature is that it supports the parallel, incremental SVD algorithms described in [8]. Since the construction of the reduced order model from the basis vectors is not a part of **libROM** and must be done by the user, we do not further discuss this library.

modred [5] is a Python library containing implementations of Proper Orthogonal Decomposition (POD) [22], balanced POD (BPOD) [38, 34], Petrov–Galerkin projection (limited only to linear systems), and Dynamic Mode Decomposition (DMD) [35]. To use **modred**, the user needs to provide (a) a vector object supporting addition and scalar multiplication; (b) a function to compute inner products; and (c) a vector handle class with a get and a set method. The authors of **modred** state in [5] that the overhead is small, and if performance becomes a problem, the user is advised to write required kernels in a compiled language (e.g., C/C++ and Fortran) and wrap them into Python modules for increased speed.

pyMOR [30] is a Python library under active development, providing reduced-basis (RB) capabilities and aims to be user friendly and easily integrable with third-party partial-differential-equations (PDE) solvers. It is similar in concept to **modred**, but it provides a more complete and robust framework. Its design is based on the observation that all high-dimensional operations in RB methods can be expressed in terms of a set of elementary linear algebra operations. **pyMOR** can be seen “as a collection of algorithms operating on **VectorArray**, **Operator**, and **Discretization** objects”, where the **Discretization** object stores the structure of a discrete problem in terms of its operators. **pyMOR** offers two main ways to be used by an application. One requires the application to output data to disk (or other persistent storage) from which **pyMOR** reads/loads what is needed. The alternative (and preferred) way requires the application to be re-compiled as a Python extension module, thus allowing **pyMOR** to access directly the application’s data structures. **pyMOR** has valuable capabilities, e.g., its own basic discretization toolkit, the ability to run the full offline phase.

pyROM [33] is a fairly recent Python framework supporting only Galerkin projection with a basis obtained via POD or DMD. The work explicitly cites **pyMOR** [30], but it does not clearly articulate how it distinguishes itself from **pyMOR**. The article states that the main operating protocol is one where **pyROM** reads data from user-supplied files; this approach is clearly not feasible for large-scale applications, where I/O is extremely expensive. Further, the work does not articulate how **pyROM** can interface with application codes written in languages other than Python.

Limitations of current approaches. We now describe our viewpoint on some weaknesses of the frameworks introduced above.

Limited to continuum systems: **modred**, **pyMOR** and **pyROM** assume an application to be expressed as a system of PDEs, and formulate their ROM methods based on the discrete system stemming from the spatial discretization of the governing PDEs. This is applicable to continuum models, but not to naturally discrete systems such as particle models.

Limited to spatial reduction: **modred**, **pyMOR** and **pyROM** support model reduction methods that reduce only the number of *spatial* degrees of freedoms. They do not support space–time techniques that enable a reduction of the number of temporal degrees of freedom [36, 39, 4, 16], which is particularly important for long-time-integration problems.

Limited to linear subspaces: **modred**, **pyMOR** and **pyROM** focus only on *linear* subspaces, without discussing potential support for *nonlinear* manifolds. This raises questions as to the extensibility of these libraries to promising recent model-reduction techniques that operate on nonlinear manifolds [19, 27].

Python as the core development language: **modred**, **pyMOR** and **pyROM** employ Python as the core development language. This seems counterintuitive, as—for performance reasons—most Python packages such as CPython, NumPy and SciPy are natively written in C, and bindings are provided to expose them to Python. This approach is also being increasingly adopted by large-scale numerical libraries, e.g., PETSc[2, 3], Trilinos². Furthermore, the authors of **modred** and **pyMOR** themselves explicitly advise users (regardless of the application’s language) to write computational kernels in a compiled language, and create wrappers to use within Python. We believe, and discuss in more detail later, that a more advantageous approach would be to use a compiled language as the core, and to create bindings to expose these functionalities in a interpreted, high-level programming language.

Need for application-specific Python bindings: Related to the item above, **modred**, **pyMOR** and **pyROM** require application-specific Python bindings for any application written in a compiled language like C/C++/Fortran or any other non-Python language. All three libraries require bindings to wrap the application’s data structures. In addition to this, **pyMOR** requires bindings to wrap the PDE-discretization operators. We believe this approach can be problematic for several reasons. First, the development of these Python bindings may be difficult or even unfeasible. This is especially true for legacy codes and more modern high performance computing (HPC)-oriented packages that use complex C++ templates and structures, like OCCA[29] or Kokkos [14]³. This is critical because, for performance reasons, most HPC applications and libraries targeting large-scale simulations are written in C, C++, or Fortran using various types of data structures. Examples include PETSc, Trilinos, Chombo, ScaLAPACK, ALGLIB, Blaze, OpenFOAM, OCCA, UPC++, mpack, NAMD, Charm++, LAMMPS, Espresso++, Gromacs, AMReX. While **pyMOR** developers offer help to integrate external PDE solvers, this can remain an obstacle for productivity due to the turnaround time of this process. The authors of **pyMOR** [30] aim to overcome this issue by shipping directly with the library suitable pre-made Python bindings for FEniCS, deal.II, Dune, and NGSolve. However, these pre-made bindings impose maintainability constraints to **pyMOR** developers, as they need to keep them up-to-date with the advancement of the corresponding libraries. Second, beside the technical challenge, the burden of writing bindings in a language different than the application’s native one could pose a productivity barrier to HPC developers. Given the choice, we believe developers would typically favor having access to libraries written in the language native to their application.

Limited applicability to modern C++ with static polymorphism: Modern C++ applications and libraries leverage compile-time (or static) polymorphism. A critical example of its use is for performance portability purposes, see e.g., OCCA, Kokkos and SYCL. These programming models are effectively built as C++ extensions, and aimed at alleviate the user from needing to know architectures-specific details to write performant code. They expose a general API allowing users to write code only once, and internally exploit compile-time polymorphism to decide on the proper data layout, and instantiate the suitable backend depending on the target threaded system,

²<https://github.com/trilinos>

³<https://github.com/kokkos>

e.g., OpenMP, CUDA, OpenCL, etc. Since Python is a dynamic language (types are inferred during interpretation), static polymorphism does not exist. Consequently, C++ applications substantially relying on static polymorphism, especially for complex use cases, would lose all its benefits if they need to interface with Python directly.

Programming model limitations: **modred**, **pyMOR** and **pyROM** omit any discussion and demonstration of their interoperability with applications exploiting emerging programming models, e.g., fully distributed task-based models and hybrid MPI+X, where X represents shared memory parallelism via threads, vectorization, tasking or parallel loop constructs. We believe that supporting interoperability with these programming models is a critical feature, because these have arisen as the leading competitors to address challenges due to hybrid architectures, increased parallelism and memory hierarchies, and will become increasingly more important.

What we propose. In this paper, we present **Pressio**⁴, a computational framework aimed at enabling projection-based model reduction for large-scale nonlinear dynamical systems. We highlight here its main features and how we believe it addresses the aforementioned limitations of existing frameworks for model reduction.

Applicable to a general ODE systems: **Pressio** provides ROM capabilities that are applicable to any system expressible as a parameterized system of ordinary differential equations (ODEs) as

$$(1.1) \quad \frac{d\mathbf{x}}{dt} = \mathbf{f}(\mathbf{x}, t; \boldsymbol{\mu}), \quad \mathbf{x}(0; \boldsymbol{\mu}) = \mathbf{x}^0(\boldsymbol{\mu}),$$

where $\mathbf{x} : [0, T] \times \mathcal{D} \rightarrow \mathbb{R}^N$ denotes the state, $\mathbf{x}^0 : \mathcal{D} \rightarrow \mathbb{R}^N$ denotes the initial state, $\boldsymbol{\mu} \in \mathcal{D} \subseteq \mathbb{R}^{n_\mu}$ denotes the system parameters, $\mathbf{f} : \mathbb{R}^N \times [0, T] \times \mathcal{D} \rightarrow \mathbb{R}^N$ with $\mathbf{f} : (\boldsymbol{\xi}, \tau, \boldsymbol{\nu}) \mapsto \mathbf{f}(\boldsymbol{\xi}, \tau, \boldsymbol{\nu})$ denotes the velocity that may be linear or nonlinear in its first argument, and $t \in [0, T]$ denotes time with $T > 0$ denoting the final time. We note that the model form (1.1) is highly expressive, as it may be derived from the spatial discretization of a PDE problem or from naturally discrete systems (e.g., molecular-dynamics problems).

Minimal API: An application needs to satisfy a minimal application programming interface (API). This consists of exposing, for a given state \mathbf{x} , time t , and parameters $\boldsymbol{\mu}$, the velocity vector $\mathbf{f}(\mathbf{x}, t; \boldsymbol{\mu})$ and the action of the Jacobian matrix $\partial \mathbf{f}(\mathbf{x}, t; \boldsymbol{\mu}) / \partial \boldsymbol{\xi}$ on a dense matrix.

Methods: **Pressio** supports model-reduction methods applicable to both steady and unsteady problems. For the latter, in particular, it provides algorithms to reduce both the spatial and temporal degrees of freedom. A detailed discussion of the supported methods is provided in § 2.

Trial manifold abstraction: We exploit software design and abstractions to generalize the concept of the trial manifold onto which the full-order model (FOM) system is projected, yielding support for both linear trial manifolds (i.e., linear trial subspaces) and nonlinear trial manifolds.

Suitable for complex nonlinear problems: **Pressio** provides ROM capabilities that are meant for complex nonlinear problems, including the least-squares Petrov–Galerkin (LSPG) projection technique [10, 9]. This technique exhibits advantages over the popular Galerkin projection because it (a) guarantees optimality of the time-discrete ROM, (b) yields smaller discrete-time *a posteriori* error bounds, (c) and often yields improved accuracy. These properties have been demonstrated for unsteady CFD applications [11, 9]. Furthermore, the LSPG method has been applied

⁴<https://github.com/Pressio>

successfully to highly nonlinear problems including transonic and hypersonic CFD cases [37, 6].

C++ core: **Pressio** is built on a C++(11) core, following a model consistent with the one used by CPython, NumPy, SciPy, as well as other HPC libraries like Trilinos and PETSc. This approach enables us to have direct integration with native C/C++ applications, and to build multiple front ends of various languages all relying on a single, compiled, optimized, and robust backend. One could argue that Fortran could have been another choice, which would bring us into a historical debate between Fortran and C/C++. We opted for C++ because (a) a substantial subset of the large-scale codes across the United States national laboratories is implemented in C++, and (b) C++ seems better suited than Fortran to design complex data structures and abstractions.

No bindings for C++ applications: Any C++ application can use **Pressio** simply as a regular library, thus avoiding any bindings. This is different than **modred**, **pyMOR** and **pyROM**, which require any C++ application to develop individual Python bindings. Eliminating the need for bindings benefits productivity which, in turn, maximizes the impact and appeal of **Pressio** not only across the national laboratories, but also on any other scientific code written in C++. We remark that this does not mean that any C++ application “magically” works with **Pressio**: as stated previously, an application must satisfy a minimal but specific API, which is discussed in § 3.1. If an application does not natively satisfy the API, its developers/users would need to expose it by working *within* the application itself using the *same* programming language. Hence, in any scenario, users and application developers operate within their domain of expertise, without needing to resort to a different language to interface to **Pressio**.

Compile-time benefits and easy deployment: **Pressio** is a header-only library written in C++(11), allowing us to fully exploit metaprogramming and perform extensive checks at *compile time*. Being header only, it does not need to be compiled, so the user can simply point to the source code, yielding a straightforward deployment.

Seamless interoperability with arbitrary programming models: **Pressio** is designed without making any assumption on the programming model or data types used by an application. Hence, it seamlessly supports arbitrary data types and arbitrarily complex programming models, e.g., MPI+X with X being a graphics processing unit (GPU), OpenMP or local tasking.

No binding code for Python applications: We leverage the modern, C++11 library **pybind11**⁵ to create Python bindings to **Pressio**. This enables any user having an application fully written in Python to use the C++ backend of **Pressio** to run ROMs. No user-defined bindings are needed (see § 3.4 for a detailed discussion). This is a key result for a two reasons. First, to support this feature, we only had to develop Python bindings in the core library *once*, which were then immediately usable by *any* Python application. Second, this exempts Python users from having to write any binding to interface with **Pressio**.

What are the drawbacks of Pressio? First, being written in C++, it is not directly usable in Fortran applications. However, as mentioned above, this can be addressed by writing Fortran bindings, as it has been done for other libraries,

⁵<https://github.com/pybind/pybind11>

e.g., `hypre`⁶ (which uses `Babel`⁷ to write its Fortran interface), and `ForTrilinos`⁸ (which is based on `SWIG`⁹).

Second, the use of metaprogramming might constitute a barrier to entry for developers who are not familiar with this technique. However, considering that generic programming is becoming increasingly more important and widespread, it is a useful skill to learn. Hence, working on **Pressio** can be advantageous for developers and, at the same time, beneficial to the actual code development.

Third, by relying on a minimal, ODE-oriented API, when a new model-reduction technique is developed, one needs to ensure (if possible) that its formulation is compatible with the same API. This might pose some limitations, e.g., for certain structure-preserving methods that leverage the underlying second-order or Hamiltonian structure [15] or the underlying finite-element [18], finite-volume [13], or discontinuous Galerkin [40] spatial discretization. In the worst case scenario, this can be addressed by augmenting the API for **Pressio** for new developments; indeed, we have already provided the required extension to enable conservative LSPG [12] for finite-volume models.

Paper organization. The paper is organized as follows. In § 2, we describe the formulation of the ROMs currently supported in **Pressio**, as well as those planned for the next release. In § 3, we discuss the implementation, the application programming interface (§ 3.1), support for arbitrary data types (§ 3.2), and the Python bindings (§ 3.4). Representative results are discussed in § 4, and conclusions in § 5.

2. Reduced-Order Models Formulation. This section presents the mathematical formulation of the ROMs currently supported in **Pressio**, as well as some details about those scheduled for integration in upcoming releases.

We consider the original computational model—which we refer to as the full-order model (FOM)—to be a dynamical system expressible as a system of parameterized ODEs of the form (1.1), which can be expressed equivalently as

$$(2.1) \quad \mathbf{r}(\dot{\mathbf{x}}, \mathbf{x}, t; \boldsymbol{\mu}) = \mathbf{0}, \quad \mathbf{x}(0; \boldsymbol{\mu}) = \mathbf{x}^0(\boldsymbol{\mu}),$$

where $\mathbf{r} : \mathbb{R}^N \times \mathbb{R}^N \times [0, T] \times \mathcal{D} \rightarrow \mathbb{R}^N$ denotes the (time-continuous) residual function defined as $\mathbf{r} := \dot{\mathbf{x}} - \mathbf{f}(\mathbf{x}, t; \boldsymbol{\mu})$.

2.1. Trial manifold. Projection-based model-reduction methods seek an approximate solution $\tilde{\mathbf{x}}(\approx \mathbf{x})$ of the form

$$(2.2) \quad \tilde{\mathbf{x}}(t; \boldsymbol{\mu}) = \mathbf{x}_{\text{ref}}(\boldsymbol{\mu}) + \mathbf{g}(\hat{\mathbf{x}}(t; \boldsymbol{\mu})),$$

where $\tilde{\mathbf{x}} : [0, T] \times \mathcal{D} \rightarrow \mathbf{x}_{\text{ref}}(\boldsymbol{\mu}) + \mathcal{M} \subseteq \mathbb{R}^N$ and $\mathcal{M} := \{\mathbf{g}(\hat{\boldsymbol{\xi}}) \mid \hat{\boldsymbol{\xi}} \in \mathbb{R}^p\} \subseteq \mathbb{R}^N$ denotes the (linear or nonlinear) trial manifold of \mathbb{R}^N . Here, $\mathbf{x}_{\text{ref}} : \mathcal{D} \rightarrow \mathbb{R}^N$ denotes a parameterized reference state and $\mathbf{g} : \hat{\boldsymbol{\xi}} \mapsto \mathbf{g}(\hat{\boldsymbol{\xi}})$ with $\mathbf{g} : \mathbb{R}^p \rightarrow \mathbb{R}^N$ and $p \leq N$ denotes the parameterization function mapping low-dimensional generalized coordinates $\hat{\mathbf{x}}$ to the high-dimensional state approximation $\tilde{\mathbf{x}}$. Henceforth, we will refer to this mapping as the “decoder” function, consistently with terminology employed in [27], where this function associated with a convolutional decoder. The approximate velocity can be obtained via chain rule yielding

$$(2.3) \quad \dot{\tilde{\mathbf{x}}}(t; \boldsymbol{\mu}) = \mathbf{J}(\hat{\mathbf{x}}(t; \boldsymbol{\mu}))\dot{\hat{\mathbf{x}}}(t; \boldsymbol{\mu}),$$

⁶<https://github.com/hypr-space/hypr>

⁷<https://computing.llnl.gov/projects/babel-high-performance-language-interoperability>

⁸<https://github.com/trilinos/ForTrilinos>

⁹<http://www.swig.org/>

where $\mathbf{J} : \hat{\boldsymbol{\xi}} \mapsto \frac{d\mathbf{g}}{d\hat{\boldsymbol{\xi}}}(\hat{\boldsymbol{\xi}})$ with $\mathbf{J} : \mathbb{R}^p \rightarrow \mathbb{R}^{N \times p}$ denoting the Jacobian of the decoder.

Linear trial manifold. When \mathbf{g} is a linear mapping, one recovers the classical affine trial subspace. In this case, the decoder can be expressed as $\mathbf{g} : \hat{\boldsymbol{\xi}} \mapsto \boldsymbol{\Phi} \hat{\boldsymbol{\xi}}$ for some trial basis matrix $\boldsymbol{\Phi} \in \mathbb{R}_*^{N \times p}$, where $\mathbb{R}_*^{n \times m}$ denotes the set of full-column-rank $n \times m$ matrices. In this case, the trial manifold is affine with $\mathcal{M} = \text{Ran}(\boldsymbol{\Phi})$ and the Jacobian a constant matrix $\mathbf{J}(\hat{\mathbf{x}}(t; \boldsymbol{\mu})) = \mathbf{J} = \boldsymbol{\Phi}$, leading to the following expression of the approximate state and velocity

$$(2.4) \quad \tilde{\mathbf{x}}(t; \boldsymbol{\mu}) = \mathbf{x}^0(\boldsymbol{\mu}) + \boldsymbol{\Phi} \hat{\mathbf{x}}(t; \boldsymbol{\mu}) \quad \text{and} \quad \dot{\tilde{\mathbf{x}}}(t; \boldsymbol{\mu}) = \boldsymbol{\Phi} \dot{\hat{\mathbf{x}}}(t; \boldsymbol{\mu}).$$

2.2. Manifold Galerkin ROM. Manifold Galerkin projection as proposed in [27] can be derived by minimizing the time-continuous residual over the trial manifold. The resulting model can be obtained by substituting the approximate state (2.2) and corresponding velocity (2.3) into Eq. (2.1), and minimizing the (weighted) ℓ^2 -norm of the resulting residual, which yields the ODE system

$$(2.5) \quad \dot{\hat{\mathbf{x}}}(t; \boldsymbol{\mu}) = \arg \min_{\hat{\mathbf{v}} \in \mathbb{R}^p} \|\mathbf{A} \mathbf{r}(\mathbf{J}(\hat{\mathbf{x}}(t; \boldsymbol{\mu})) \hat{\mathbf{v}}, \mathbf{x}_{\text{ref}}(\boldsymbol{\mu}) + \mathbf{g}(\hat{\mathbf{x}}(t; \boldsymbol{\mu}), t; \boldsymbol{\mu}))\|_2^2,$$

which can be written equivalently as

$$(2.6) \quad \dot{\hat{\mathbf{x}}}(t; \boldsymbol{\mu}) = (\mathbf{A} \mathbf{J}(\hat{\mathbf{x}}(t; \boldsymbol{\mu}))^\dagger \mathbf{A} \mathbf{f}(\mathbf{x}_{\text{ref}}(\boldsymbol{\mu}) + \mathbf{g}(\hat{\mathbf{x}}(t; \boldsymbol{\mu}), t; \boldsymbol{\mu})),$$

where the superscript $+$ denotes the Moore–Penrose pseudoinverse, $\hat{\mathbf{x}}(0; \boldsymbol{\mu}) = \hat{\mathbf{x}}^0(\boldsymbol{\mu})$ is the reduced initial condition (e.g., computed by performing orthogonal projection of the $\mathbf{x}^0(\boldsymbol{\mu})$ onto the trial manifold [27]), and $\mathbf{A} \in \mathbb{R}^{z \times N}$ with $z \leq N$ is a weighting matrix that enables the definition of a weighted (semi)norm. The ODE system (2.6) can be integrated in time using any time stepping scheme.

If we select the $N \times N$ identity matrix, i.e. $\mathbf{A} = \mathbf{I}$, the projection is typically insufficient to yield computational savings when the velocity is nonlinear in its first argument, as the N -dimensional nonlinear operators must be repeatedly computed, thus precluding an N -independent online operation count. To overcome this computational bottleneck, one can choose \mathbf{A} to have a small number of nonzero columns. When the residual Jacobian is sparse, this sparsity pattern leads to “hyper-reduction”, which yields an N -independent online operation count by approximating the nonlinear operators by computing a small (N -independent) subset of their elements. Examples include collocation, i.e., $\mathbf{A} = \mathbf{P}$ with \mathbf{P} comprising selected rows of the identity matrix, and the GNAT method [10, 11], i.e., $\mathbf{A} = (\mathbf{P} \boldsymbol{\Phi}_r)^\dagger \mathbf{P}$ with $\boldsymbol{\Phi}_r \in \mathbb{R}_*^{N \times z}$ comprising a basis matrix for the residual.

Manifold Galerkin is currently supported in **Pressio** for both linear and nonlinear trial manifolds. For the linear case, the user needs to provide the constant basis matrix $\boldsymbol{\Phi}$. For the nonlinear case, the user is responsible for implementing the decoder mapping \mathbf{g} , which **Pressio** uses without knowledge of its implementation details. In a future release, we plan to add support for a set of default choices for nonlinear mappings, e.g., convolutional autoencoders as in [27]. For the weighting matrix, we currently support $\mathbf{A} = \mathbf{I}$, the collocation-based hyper-reduction $\mathbf{A} = \mathbf{P}$, and an arbitrary weighting matrix specified by the user, while the GNAT-based weighting matrix $\mathbf{A} = (\mathbf{P} \boldsymbol{\Phi}_r)^\dagger \mathbf{P}$ is under development.

2.3. Manifold Least-squares Petrov–Galerkin (LSPG) ROM. In contrast to Galerkin projection, LSPG projection corresponds to minimizing the (weighted) ℓ^2 -norm of the *time-discrete* residual over the trial manifold. Hence, the starting point for

this approach the residual ODE formulation (2.1) discretized in time with an arbitrary time-discretization method. Here, we focus on *implicit* linear multistep methods for two primary reasons: first, Galerkin and LSPG are equivalent for explicit schemes [9]; second, at the time of this writing, implicit linear multistep schemes are the main implicit schemes supported in **Pressio**. Other families of time stepping schemes, e.g., diagonally implicit Runge–Kutta, will be supported in future developments; [9] describes LSPG for Runge–Kutta schemes in detail.

A linear k -step method applied to numerically solve the problem (1.1) leads to solving a sequence of systems of algebraic equations

$$(2.7) \quad \mathbf{r}^n(\mathbf{x}^n; \boldsymbol{\mu}) = \mathbf{0}, \quad n = 1, \dots, N_t,$$

where N_t denotes the total number of instances, \mathbf{x}^n denotes the state at the n th time instance, and $\mathbf{r}^n : \mathbb{R}^N \times \mathcal{D} \rightarrow \mathbb{R}^N$ denotes the *time-discrete* residual. At the n -th time instance, we can then write:

$$(2.8) \quad \alpha_0 \mathbf{x}^n - \Delta t \beta_0 \mathbf{f}(\mathbf{x}^n, t^n; \boldsymbol{\mu}) \sum_{j=1}^k \alpha_j \mathbf{x}^{n-j} \Delta t \sum_{j=1}^k \beta_j \mathbf{f}(\mathbf{x}^{n-j}, t^{n-j}; \boldsymbol{\mu}) = \mathbf{0},$$

where $\Delta t \in \mathbb{R}_+$ denotes the time step, \mathbf{x}^k denotes the numerical approximation to $\mathbf{x}(k\Delta t; \boldsymbol{\mu})$, the coefficients α_j and β_j , $j = 0, \dots, k$ with $\sum_{j=0}^k \alpha_j = 0$ define a particular multistep scheme, and $\beta_0 \neq 0$ is required for implicit schemes. For simplicity, we assume a uniform time step Δt and a fixed number of steps k for each time instance, but extensions to nonuniform time grids and a non-constant value of k are straightforward. For example, setting $k = 1$ and $\alpha_0 = \beta_0 = 1$, $\alpha_1 = -1$, $\beta_1 = 0$, yields the backward Euler method.

LSPG projection is derived by substituting the approximate state (2.2) in the time-discrete residual (2.7) and minimizing its (weighted) ℓ^2 -norm, which yields a sequence of residual-minimization problems

$$(2.9) \quad \hat{\mathbf{x}}^n(\boldsymbol{\mu}) = \arg \min_{\hat{\mathbf{x}} \in \mathbb{R}^p} \left\| \mathbf{A} \mathbf{r}^n \left(\mathbf{x}_{\text{ref}}(\boldsymbol{\mu}) + \mathbf{g}(\hat{\mathbf{x}}; \boldsymbol{\mu}) \right) \right\|_2^2, \quad n = 1, \dots, N_t$$

with initial condition $\hat{\mathbf{x}}(0; \boldsymbol{\mu}) = \hat{\mathbf{x}}^0(\boldsymbol{\mu})$. As in § 2.2, $\mathbf{A} \in \mathbb{R}^{z \times N}$ with $z \leq N$ denotes a weighting matrix that can enable hyper-reduction.

LSPG formulation for stationary problems. Manifold LSPG can be applied to steady-state problems by computing $\mathbf{x}(\boldsymbol{\mu})$ as the solution to Eq. (1.1) with $\dot{\mathbf{x}} = \mathbf{0}$, which yields

$$(2.10) \quad \mathbf{f}(\mathbf{x}; \boldsymbol{\mu}) = \mathbf{0},$$

where the time-independent velocity is equivalent to the residual of the stationary-problem. Substituting the approximate state (2.2) into Eq. (2.10) and minimizing the ℓ^2 -norm of the residual yields

$$(2.11) \quad \hat{\mathbf{x}}(\boldsymbol{\mu}) = \arg \min_{\hat{\mathbf{x}} \in \mathbb{R}^p} \left\| \mathbf{A} \mathbf{f} \left(\mathbf{x}_{\text{ref}}(\boldsymbol{\mu}) + \mathbf{g}(\hat{\mathbf{x}}; \boldsymbol{\mu}) \right) \right\|_2^2,$$

which has the same nonlinear-least-squares form obtained for a time-dependent problem shown in Eq. (2.9).

Constrained LSPG formulation. If the minimization problems (2.9) and (2.11) are equipped with constraints, one obtains unsteady and steady constrained LSPG problems, respectively. An example within this category of models is the conservative LSPG formulation in [13], which ensures the reduced-order model is conservative over subdomains of the problem in the case of finite-volume discretizations. This method relies on a nonlinear equality constraint to enforce conservation. The reader is referred to [13] for additional details on conservative LSPG projection, including feasibility conditions of the associated optimization problems, and error bounds.

Pressio supports manifold LSPG and conservative LSPG for both steady and unsteady problems. As with manifold Galerkin projection, it supports weighting matrices $\mathbf{A} = \mathbf{I}$, the collocation-based hyper-reduction approach $\mathbf{A} = \mathbf{P}$, or an arbitrary weighting matrix specified by the user. Native support for the GNAT-based weighting matrix is under development.

2.4. Space–time model reduction. In § 2.2 and § 2.3, we presented ROMs that reduce the *spatial* dimensionality of a dynamical system; this yields a ROM that still needs to be resolved in time via numerical integration. In some cases, the reduced system can be integrated with a time step larger than the one used for the full-order model, see [1]. However, this still imposes a limitation to the achievable computational savings. To address the time dimension directly, one can employ space–time model-reduction methods that simultaneously reduce both the number spatial and temporal degrees of freedom of the ODE system. To address this need, we are currently implementing in **Pressio** the space–time least-squares Petrov–Galerkin (ST-LSPG) projection method [16] and the windowed least-squares (WLS) method [32]. Because these techniques will be released in the future, we briefly describe here the main idea behind them, but omit the full mathematical details. For a complete formulation of ST-LSPG and WLS, the reader is directed to the aforementioned references.

ST-LSPG relies on a low-dimensional space–time trial manifold, which—in the case of a linear space–time trial manifold—can be obtained by computing tensor decompositions of snapshot matrices constructed from spatio-temporal state data. The method then computes discrete-optimal approximations in this space–time trial subspace by minimizing the (weighted) ℓ^2 -norm of the space–time residual, which corresponds to the concatenation of the time-discrete residual over all time steps.

The windowed least-squares (WLS) [32] method is a model-reduction approach comprising a generalization of Galerkin, LSPG, and ST-LSPG. WLS operates by sequentially minimizing the dynamical system residual within a low-dimensional trial manifold over time windows. WLS can be formulated for two types of trial manifolds: *spatial trial manifolds* that reduce the spatial dimension of the full-order model, and *space–time trial manifolds* that reduce the spatio-temporal dimensions of the full-order model.

3. Pressio. The core component of **Pressio** is a C++(11) header-only library that leverages generic programming (i.e., templates) to enable support for native C++ applications with arbitrary data types. Metaprogramming is used for type checking and introspection, to ensure that types are compatible with the design and requirements. Being header-only, **Pressio** does not need to be separately compiled, packaged, or installed; the user must only point to the source code. The development is based on the following objectives: (a) support for general computational models (data structures, problem types), (b) heterogeneous hardware (many-core, multi-core, accelerators), (c) performance, and (d) extensibility. The key advantage of having a single framework is that when a new method is developed, it can be immediately

used by any application already using **Pressio**. **Pressio** is modularized into separate packages as follows:

- **mpl**: metaprogramming functionalities
- **utils**: common functionalities, e.g., I/O helpers, static constants, etc.
- **containers**: data structures
- **ops**: linear algebra operations
- **qr**: QR factorization functionalities
- **svd**: singular value decomposition (SVD) functionalities
- **solvers**: linear and nonlinear solvers
- **ode**: explicit and implicit time steppers and integrators
- **rom**: reduced-order modeling methods

The order used above is informative of the dependency structure. For example, every package depends on **mpl**, but **qr** depends only on **mpl**, **utils**, **containers**. The **rom** package resides at the bottom of the hierarchy and depends on the others. Each package contains corresponding unit and regression tests.

3.1. What API does Pressio require from an external application? The design of **Pressio/rom** is based on the observation that all methods listed in § 2 can be applied to any dynamical system of the general form (2.1), and only require access to the velocity, \mathbf{f} , and the *action* of the Jacobian matrix $\partial \mathbf{f} / \partial \boldsymbol{\xi}$, on an operand, \mathbf{B} , which is a tall, skinny matrix (e.g., the decoder Jacobian $d\mathbf{g} / d\boldsymbol{\xi}$). Querying the action of the Jacobian on an operand rather than the Jacobian itself is essential, because in many applications the Jacobian itself cannot easily be explicitly assembled or stored.

We envision two scenarios: one in which an application natively supports the above functionalities, and one in which it does not. In the first scenario, minimal work (e.g., rearranging some functions in the native code) is needed to adapt the application to use **Pressio/rom**. We believe this best case scenario to be a reasonable expectation from applications using expressive syntax, well-defined abstractions and encapsulation. These software engineering practices guide developers to design codes using proper abstractions directly expressing the target mathematical concept. For systems of the form (2.1), this means implementing the velocity \mathbf{f} as a self-contained free function or as a class method encapsulating the implementation details. This kind of abstraction and design would satisfy the best practices for software engineering and also naturally fits our expressive API model. To further emphasize this point, we remark that the same expressive model is being used/expected by other well-established libraries, e.g., Sundials[21], SciPy.ode. If an application needs to be interfaced with these libraries, the developers would need to meet a similar, expressive, intuitive API designed for dynamical systems.

When an application does not readily expose the required functionalities, the user or developer needs to expose them. This can be done, e.g., by writing an adapter class inside the application. Even for this scenario, we argue that the effort needed is easily manageable, and even useful, for the following reasons: (a) the adapter class needs to be developed using the same language of the application; (b) to write the adapter, a developer/user would still operate within their domain of knowledge; and (c) once this adapter class is complete, the application would gain (almost) seamless compatibility with other libraries targeting dynamical systems since most of them are based on the same API model.

Figure 1 shows a schematic of the interaction between **Pressio/rom** and a generic application. The application owns the information defining the problem, i.e., the parameters $\boldsymbol{\mu}$, mesh, inputs, etc.. **Pressio** is used as an external library, and the in-

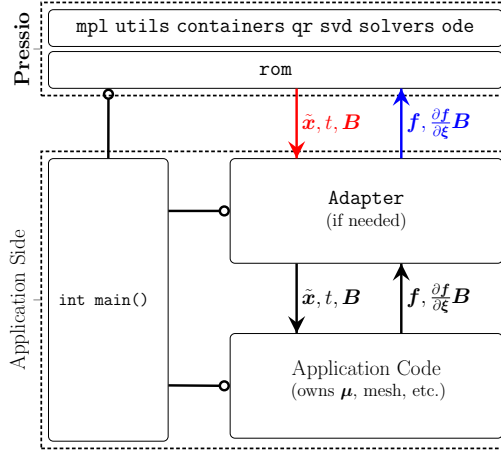


FIG. 1. Schematic of the interaction between **Pressio** and the application, highlighting elements belonging to **Pressio** and those belonging to the application. The solid, black line (—o) indicates that the main function is where all the various components are used. The red arrow is used to indicate information/data computed by and exiting **Pressio**, while blue is used to denote information/data computed by the application and entering **Pressio**. For a steady problem, the schematic would be similar without the time dependence.

teraction can be seen simply as an exchange of information: for a given approximate state $\tilde{\mathbf{x}}$, time t , and operand \mathbf{B} , **Pressio/rom** queries the application for the associated velocity $\mathbf{f}(\tilde{\mathbf{x}}, t; \boldsymbol{\mu})$ and Jacobian action $\frac{\partial \mathbf{f}}{\partial \boldsymbol{\xi}}(\tilde{\mathbf{x}}, t; \boldsymbol{\mu})\mathbf{B}$. In the schematic, a red arrow indicates the information/data exiting **Pressio** and entering the application, while a blue arrow denotes the reverse. If the adapter is not needed, then **Pressio** interacts directly with the core application classes. When the problem is steady, time dependency simply drops.

Listing 1 shows an example of a valid C++ adapter class satisfying the API for Galerkin and LSPG for unsteady problems. The listing shows four type aliasing declarations and four methods. If any of them are missing, or the syntax shown is not met exactly, a compile-time error is thrown. This static checking allows us to ensure the correctness of the API. For performance reasons, the non-void methods are only called once during the setup stage to copy construct the objects. More details on the overall software design are presented in the supplementary material.

All the methods are `const`-qualified to ensure const-correctness. **Pressio** does not cast away the `const` qualification of the adapter/application object to preserve its visibility. The user can choose to implement the adapter class’ methods such that no modification happens for the data members, or explicitly use the `mutable` C++ keyword. The `mutable` keyword allows one to qualify data members that can be modified within those `const`-qualified methods. This is typically used for cases, like this one, where one may have to mutate the state for an implementation detail, while keeping the visible state of an object the same.

The adapter class’ methods accept arguments by reference to avoid (potentially) expensive copies of large objects. If an application relies on data structures with “view semantics”, see e.g., Kokkos or Tpetra in Trilinos, the user can simply omit the references in the arguments of the adapter class methods. View semantics means that an assignment operator performs a shallow-copy operation, i.e., only the memory reference and dimensions are copied. View semantics thus behave like the C++ shared

LISTING 1

Skeleton C++ adapter class satisfying the unsteady API for Galerkin and LSPG ROMs.

```

1  class SampleAdapterClass{
2      //...
3  public:
4      /* C++11 type aliasing declarations that Pressio detects */
5      /* this is equivalent to doing: typedef ... scalar_type */
6      using scalar_type      = /*application's scalar type      */;
7      using state_type       = /*          state type          */;
8      using velocity_type    = /*          velocity type        */;
9      using dense_matrix_type = /*          dense matrix type   */;
10     //...
11
12     // compute velocity, f(x,t;...), for a given state, x(t)
13     void velocity(const state_type & x,
14                  const scalar_type & t,
15                  velocity_type & f) const;
16
17     // given current state x(t):
18     // 1. compute the spatial Jacobian, df/dx
19     // 2. compute A=df/dx*B, B is typically a skinny dense matrix
20     void applyJacobian(const state_type & x,
21                      const dense_matrix_type & B,
22                      const scalar_type & t,
23                      dense_matrix_type & A) const;
24
25     // overload called once to construct an initial object
26     velocity_type velocity(const state_type & x,
27                          const scalar_type & t) const;
28
29     // overload called once to construct an initial object
30     dense_matrix_type applyJacobian(const state_type & x,
31                                   const dense_matrix_type & B,
32                                   const scalar_type & t) const;

```

pointer semantics. While it would still work to accept by reference objects of types with view semantics, it would be more appropriate to pass them by copy to ensure proper reference counting.

3.2. How does Pressio handle arbitrary data structures? Support for arbitrary data types is enabled via generic programming and type introspection. Generic programming (i.e., C++ templates) implies that, implementation-wise, **Pressio** can naturally accomodate arbitrary types. Quoting from [31]: “Generic programming centers around the idea of abstracting from concrete, efficient algorithms to obtain generic algorithms that can be combined with different data representations to produce a wide variety of useful software”. Broadly speaking, we can say that **Pressio** contains algorithms and operations written abstractly as high-level steps to operate on a generic type. This, however, is a necessary but not sufficient condition to enable arbitrary types. It is clear, in fact, that some class or functions templates performing specific operations are applicable only to types satisfying certain conditions. This is where type introspection comes into play.

Type introspection allows the examination of a type to analyze its properties at compile-time using metaprogramming techniques. This is the foundation of design by introspection, a programming paradigm that relies on performing introspection on components and making decisions during compilation. For the sake of argument, think of a function template applicable only to types that can be default constructed. Introspection can be used to examine the template argument to detect if it is default constructible, and differentiate code according to whether this property is satisfied or not. Another example is the ability to selectively enable/disable functions or classes based on whether the corresponding template arguments satisfy some requirements.

The above approach is not exclusive to achieve support for arbitrary types. One possible alternative is based on inheritance and dynamic polymorphism. In this case, the library would contain specific base (or abstract) classes to represent well-defined interfaces for target functionalities. These abstract classes are used via dynamic polymorphism inside the algorithms. Users would be able to employ their data types by inheriting from the base classes, thus creating new types that are fully compatible with the library algorithms. This is a valid approach, but has some disadvantages: (a) templates and type introspection is an approach more suitable than inheritance to obtain type safety; (b) dynamic polymorphism has an overhead (due to a virtual table lookup) for each function invocation; (c) type introspection fully exploits the power of templates, which is a key feature of C++; (d) design by introspection will become even more natural to adopt and use when C++ concepts become part of the standard.

Pressio performs introspection on the types instantiated by the user and, therefore, can decide at compile-time to select specialized implementations of type-specific algebra operations. To this end, we have implemented in **Pressio** a suite of pre-defined implementations of basic algebra operations for several widely-used libraries, e.g., Trilinos, Kokkos, Eigen, Armadillo. Additional implementations for other packages, like PETSc and hypre, are planned for upcoming releases. Whenever possible, **Pressio** exploits the implementations native to the target libraries to perform all operations. This approach allows us to fully exploit the native performance of these libraries benefiting from the substantial amount of work done to achieve optimal performance in these libraries. If an external application uses a custom set of data structures and operations, or if types-specific operations are not already supported in **Pressio**, the user needs to provide a class implementing specific operations needed to carry out all of the necessary ROM computations, e.g., dot products, matrix-vector and matrix-matrix products. One advantage of this approach is that, if needed, the user can “plug-and-play” and test various implementations of the low-level algebra operations.

While this approach might resemble the one in **modred**, **pyMOR** and **pyROM**, we highlight the following differences. **modred**, **pyMOR** and **pyROM** require C/C++/Fortran users to write custom Python—which is not the native application’s language—bindings to wrap their application’s data structures. In addition, **pyMOR** needs bindings to wrap the application’s PDE operators. **Pressio**, on the contrary, does not need bindings for the application’s data structures, since these just become template arguments. Also, **Pressio** only requires (in certain cases) a single class containing a small set of basic algebra operations. We stress that this class with algebra operations requires little effort from the user, because (a) it is written in the application’s native language; and (b) it simply involves forwarding calls to operations and methods already implemented by the application’s native data structures. Finally, **Pressio** does not need any information about the application’s spatial oper-

ators or discretization. This stems from the fact that the ROMs in **Pressio** are only based on the assumption that a target system is represented as a system of ODEs.

3.3. How does Pressio support hyper-reduction? The notion of hyper-reduction (or sample mesh) was introduced in § 2, and consists of approximating the nonlinear operators (residual and, if needed, the Jacobian) of the full order model by sampling only a subset of elements. Equipping a ROM with this technique yields large computational savings, see e.g., [11], and is thus a critical component. A detailed description and comparison of various hyper-reduction techniques can be found in [11].

In **Pressio**, one can explore the effects of hyper-reduction in two ways. The first, which we refer to as “algebraic hyper-reduction”, requires the user to simply provide the desired weighting matrix, \mathbf{A} , which **Pressio** applies to the FOM operators to extract the target subset of elements. The immediate benefit is a much smaller nonlinear minimization problem to solve, see Eqs. (2.5), (2.9) and (2.11). While easy to implement, the main drawback is that the FOM still needs to compute the full operators, whose cost typically dominates the cost to solve the minimization problem. This implies that one cannot expect to obtain substantial savings. Hence, the algebraic hyper-reduction allows one to just *mimic* the effect of a real implementation.

The second (preferred) way requires an application to have the capability of evaluating the nonlinear operators *only* at target locations of the mesh, i.e., a “sample mesh”. This scenario considerably reduces the cost of evaluating the FOM’s operators, thus accentuating the benefits of hyper-reduction, see e.g., [6]. This second approach, however, is strictly dependent on the application’s numerical method and mesh, and thus needs to be implemented by the user directly within the application. We remark, however, that while this task can be intrusive, it is paradoxically easier to implement for complex applications, e.g., those based on an unstructured mesh. On the one hand, the complexity of these meshes is a disadvantage because one has to specify the full connectivity between the elements. On the other hand, the complexity of an unstructured mesh is an advantage because it allows more freedom in how the elements are assembled, which clearly benefits the construction of the sample mesh. This will be further discussed in § 4.1 in relation to one of our test cases.

3.4. pressio4py. To increase the impact and widen the range of potential users of **Pressio**, we have developed **pressio4py**¹⁰, a library of Python bindings to **Pressio**. **pressio4py** is implemented using **pybind11** [24], a lightweight open-source library that leverages C++11 and metaprogramming to facilitate the interoperability between C++ and Python. The objective of **pressio4py** is twofold. First, to allow *any* Python application based on NumPy to use the capabilities in **Pressio** without any additional glue code. The only requirement is that the Python application meets an API similar to the one shown in listing 1. Second, to enable a Python application to obtain a performance comparable to the one obtained with a C++ application natively interfacing with **Pressio**.

Developing **pressio4py** has required minimal effort, mostly in the form of add-on functionalities needing minor modifications to the core C++ **Pressio** code. This is a result of two main factors, namely the quality and ease of use of **pybind11**, and the modularity of **Pressio**, which allowed us to develop extensible and maintainable bindings relatively quickly and easily. More specifically, the work involved two main stages. One aimed at enabling **Pressio** to support `pybind11::array_t`. The latter is a class template in **pybind11** to bind a NumPy array from the C++ side. Using

¹⁰<https://github.com/Pressio/pressio4py>

LISTING 2

*Sample Python adapter class satisfying the API for **pressio4py**.*

```

1 class Adapter:
2     def __init__(self, *args):
3         # initialize (if needed)
4         # create velocity vector, f, and Jacobian matrix, Jac
5
6     # compute velocity, f(x,t;...), for a given state, x
7     def velocity(self, x, t):
8         # compute f (here f is a member of the class)
9         return self.f
10
11     # given current state x(t):
12     # 1. compute the spatial Jacobian, df/dx
13     # 2. compute A=df/dx*B, B is typically a skinny dense matrix
14     def applyJacobian(self, x, B, t):
15         # compute Jac = df/dx (here Jac is a member of the class)
16         # Jac is typically sparse, so we use Jac.dot(B)
17         # When Jac is dense, use np.matmul(Jac,B)
18         return self.Jac.dot(B)

```

`pybind11::array_t` allows us to optimize interoperability with Python since no copy needs to occur when a NumPy array from the Python side is passed to a C++ function accepting a `pybind11::array_t`. This also allows us to bypass the Python interpreter, and perform all operations by working directly on the underlying data, thus yielding a negligible overhead. A key property of `pybind11::array_t` is that it has view semantics and, therefore, special attention is needed depending on whether a deep or shallow copy is needed. To achieve this, we leverage type introspection allowing **Pressio** to support `pybind11::array_t` in a straightforward and natural way. The second stage of the work involved developing the actual **pybind11**-based binding code to expose the **Pressio** functionalities to Python. This stage benefited from the ease of use and power of **pybind11**, which is written to naturally target C++ and, in most situations, leading to simple binding code. This is what we observed for **Pressio**. For example, the binding code to expose the basic LSPG functionalities is less than 100 lines.

Listing 2 shows an example of a Python class satisfying the API for **pressio4py**, revealing clear similarities with the C++ listing 1. When instantiating a ROM problem, the user can decide to provide an object with custom algebra operations (e.g., to specify how to perform matrix-vector products) for **pressio4py** to use where needed, or let **pressio4py** rely on default implementation of these operations. In the latter scenario, **pressio4py** operates by making direct calls to NumPy and SciPy functionalities to act directly on `pybind11::array_t` data. This is enabled by importing the NumPy or SciPy modules *directly* inside the C++ code as `pybind11::objects`. For example, if we need to compute a on-node matrix-vector product, we obtain optimal performance by calling the Blas function `dgemv` to operate directly on the underlying matrix and vector data. One scenario where this is not entirely possible is when a user wants to run a ROM with hyper-reduction. In this case, the user is required to provide custom functionalities, namely the computation of the time-discrete operators. Nothing else changes as far as matrix and vector manipulations since these

low-level operations are still handled by `pressio4py`.

4. Results. This section aims at demonstrating the use of **Pressio** in two different scenarios: in § 4.1, we discuss the application of the LSPG ROM to a large-scale simulation of a hypersonic-flow problem, while in § 4.2 we discuss overhead and performance of `pressio4py`.

4.1. LSPG ROM for hypersonics. This section presents representative results obtained using SPARC (Sandia Parallel Aerodynamics and Reentry Code). SPARC is a Computational Fluid Dynamics (CFD) code implemented in C++ for solving aerodynamics and aerothermodynamics problems. It solves the compressible Navier–Stokes and Reynolds-averaged Navier–Stokes (RANS) equations on structured and unstructured grids using a cell-centered finite-volume discretization scheme, and the transient heat and associated equations for non-decomposing and decomposing ablators on unstructured grids using a Galerkin finite-element method [23]. SPARC relies on the distributed numerical linear algebra data structures in Tpetra which, in turn, leverages the Kokkos programming model to achieve performance portability across next-generation computing platforms. The reader is referred to [23] for details on the governing equations and code design of SPARC.

The version of SPARC we used for our test did not natively expose the API needed by **Pressio** shown in 1. However, its modular design made the implementation of an adapter class quite straightforward. In fact, the “velocity” and the evaluation of the Jacobian functionalities were already present within SPARC—used by the native code within each nonlinear solver iteration—despite being buried within a few abstraction layers. Therefore, we just needed to create an adapter class bypassing these layers and accessing these functionalities directly. Having access to the spatial Jacobian, computing the `applyJacobian` required by **Pressio** (see 1) was straightforward because it simply involved calling a method of the native Jacobian’s data structure to compute its action on the operand **B**. Overall, we can say that implementing the adapter class was quite easy, requiring no modifications to the core SPARC code, but just the addition of a few methods including those to initialize the discretization, read in basis vectors, and post-process the ROM results. This experience is an example of what was discussed in § 3.1, i.e., an application that, despite being complex, required only minor effort to interface with **Pressio** due to its modular and extensible design.

As a test case, we choose a CFD simulation of the Blottner sphere, a commonly used validation case for hypersonic CFD solvers [7]. It models a hypersonic flow impacting on a semi-sphere similar to the round tips commonly found on hypersonic aircraft and spacecraft. A schematic of the problem is shown in Figure 2 (a). The main feature is the bow shockwave just upstream of the sphere, which can be difficult to capture accurately due to the shock strength and a numerical phenomena known as the carbuncle problem [28]. Non-dimensional quantities characterizing the problem are the Mach number, $M = 5.0$, and the Reynolds Number, $Re = 1,887,500$. Despite the large Reynolds number, this problem is run without a turbulence model, and the boundary layer is assumed to be laminar [7].

The FOM is based on a spatial discretization using a structured mesh with 4,192,304 cells shown in Figure 2 (b). The mesh is designed so that the cells are well aligned with the bow shock and the boundary layer on the sphere surface, and it extends upstream enough to capture the bow shock but not so far so as to control the cell count. Since the flow is modeled as laminar, there are 5 conserved quantities, yielding the total FOM degrees of freedom to be $N = 20,971,520$. We focus on the pseudo-transient behavior of the system from a uniform $M = 5.0$ flow to steady state.

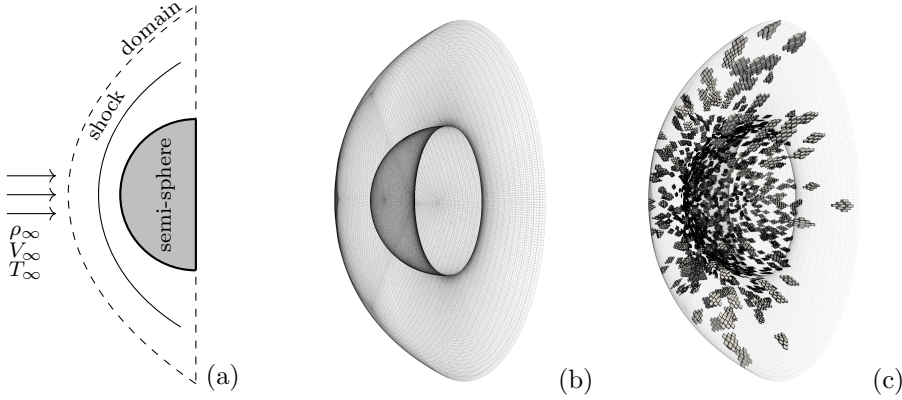


FIG. 2. Panel (a): schematic of Blottner sphere, where ρ_∞ , V_∞ and T_∞ refer to the free-stream density, velocity and temperature, respectively. The computational domain is displayed with a dashed line. The bow shock to the left of the semi-sphere is where the hypersonic airflow almost suddenly decelerates to subsonic velocity, with density and temperature increasing near the sphere surface. Note that the schematic is shown in two dimensions for clarity, but the actual simulation is fully three-dimensional. Panel (b): angled front view of the full 3D mesh used for the full-order model of the Blottner sphere. Panel (c): angled front view of one of the sample meshes used to run the ROMs with hyper-reduction, which is composed of 1,678 randomly selected cells in which the residual is sampled, along with neighboring cells and neighbors of neighbors, yielding 41,414 cells in total, equivalent to $\sim 1\%$ of the full mesh.

The pseudo time stepping is performed using the (implicit) backward Euler scheme with fixed time step $\Delta t = 2.5 \times 10^{-6}$ seconds, yielding 64 time instances. At each time instance, the nonlinear system resulting from the implicit time discretization is solved using a Newton–Raphson solver until the ℓ^2 -norm of the residual is reduced by three orders of magnitude [23]; the initial guess is taken to be the solution at the previous time instance. During the pseudo-transient phase, the bow shock upstream of the sphere moves and deforms until it reaches a steady state.

We consider the LSPG method described in § 2.3 with a linear trial subspace, and limit the study to a reproductive ROM. This means that we fix the system parameters μ —which in this case correspond to boundary conditions and physical constants—and assess the ability of the ROM to reproduce the FOM results. A predictive ROM study is outside the scope of the present work, and we refer the reader to [6] for a paper showing ROMs developed in **Pressio** yielding good performance in a predictive setting for a hypersonic-flow problem. To compute the basis matrix Φ , we take snapshots of the full-order model state at all 64 time instances, subtract the initial condition $\mathbf{x}^0(\mu)$ from each snapshot, and compute the corresponding POD modes. We consider four cases, namely $p = 8, 16, 32$, and 64 modes. For the ROM, we use the same time discretization method and time step size as the FOM. The LSPG minimization problem in Eq. (2.9) employs $\mathbf{x}_{\text{ref}} = \mathbf{x}^0$ and is solved using the Gauss–Newton method solver implemented in **Pressio** that assembles and solves the normal equations, terminating when the ℓ^2 -norm of the normal-equations relative residual is reduced by three orders of magnitude; the initial guess is taken to be the solution at the previous time instance. We consider two different choices of the weighting matrix \mathbf{A} for the problem in Eq. (2.9):

1. *Diagonal matrix without hyper-reduction:* we choose $\mathbf{A} = \mathbf{D} \in \mathbb{R}^{N \times N}$, where $\mathbf{D} \in \mathbb{R}^{N \times N}$ is a diagonal matrix whose elements correspond to the sizes of the control volumes in the finite-volume discretization divided by the time step Δt . We found that

this choice of \mathbf{A} greatly improves the convergence rate of Gauss–Newton iterations. This case is useful for demonstration purposes but is expected not to yield substantial computational savings because no hyper-reduction is employed. For brevity, below we refer to this case with the abbreviation sm_{100} to indicate that this uses 100% of the full mesh.

2. *Diagonal matrix with collocation hyper-reduction:* we choose $\mathbf{A} = \mathbf{P}\mathbf{D} \in \mathbb{R}^{z \times N}$, where $\mathbf{D} \in \mathbb{R}^{N \times N}$ is the same as the case above, and the sample matrix $\mathbf{P} \in \{0, 1\}^{z \times N}$ corresponds to $z (\ll N)$ randomly selected rows of the identity matrix. Note that, as suggested in [11], this random sampling is done such that we obtain cells at each boundary. To enable this in SPARC we use a sample mesh. The main difficulty of using a sample mesh stems from the need to perform computations on its odd topology comprised of disjoint sets of cells. However, this proved relatively easy in SPARC because of its support for unstructured meshes—specifically those in the EXODUS II¹¹ file format [23]. Data structures for unstructured meshes are, in fact, well-suited to handle a sample mesh (as anticipated in § 3.3), because they hold, for every cell of the domain, the full connectivity list and faces corresponding to side sets. Therefore, SPARC did not have to be modified to perform computations on a sample mesh. This confirms our statement in § 3.3: implementing hyper-reduction for unstructured meshes is, in general, relatively straightforward. In this work, we explore sample meshes corresponding to 1%, 2%, 5%, and 10% of the full mesh, and we refer to them with the symbols sm_1 , sm_2 , sm_5 and sm_{10} , respectively. A visualization of the sample mesh containing 1% of the full mesh is shown in Figure 2 (c).

All of the results presented below for the Blottner sphere are run on a Sandia cluster containing a total of 1,848 nodes with Infiniband interconnect, each node having two 8-core Intel(R) Xeon(R) CPU E5-2670 0 @ 2.60GHz and 65GB of memory. To run a FOM simulation, we use 512 MPI processes, distributed over 32 nodes. This configuration follows SPARC’s requirements and allows us to balance the memory footprint of the application. The hyper-reduced ROMs run on a single node, since the sample mesh is small enough. The mesh for the ROM without hyper-reduction is distributed using the same number of nodes used for the FOM. We choose Kokkos for the ROM data structures and computations. This is advantageous for two main reasons: first, it yields seamless interoperability with the Tpetra-based data structures of SPARC; second, it allows us, in the future, to tackle more complex SPARC problems by leveraging on-node threading models or directly on the GPU without modifying the code. In this work, Kokkos is built with a serial backend. A detailed study comparing various threading models for running the ROM is left to future work.

Accuracy: Figure 3 shows representative visualizations of the flow, color-coded by the Mach number, and the sphere surface, color-coded by the local heat flux. The plots show that the ROM faithfully captures the bow shock and high heating around the flow stagnation point, yielding differences with the FOM that are nearly indistinguishable. To quantify these differences, we report in Table 1 the relative errors of the ROM with respect to the FOM measured in the discrete ℓ^2 - and ℓ^∞ -norms for the state vector on the entire computational domain, and vectors containing the wall heat flux and wall shear stress at all surface cell faces. For each sample mesh except sm_1 , the error decreases monotonically with the reduced dimension p (i.e., the number of basis vectors). We emphasize that as the reduced dimension increases, monotonic decrease in the errors reported here is not guaranteed, even when full mesh sampling is used. Overall, we can say that for all configurations explored, the ROM

¹¹<https://gsjaardema.github.io/seacas/html/index.html>

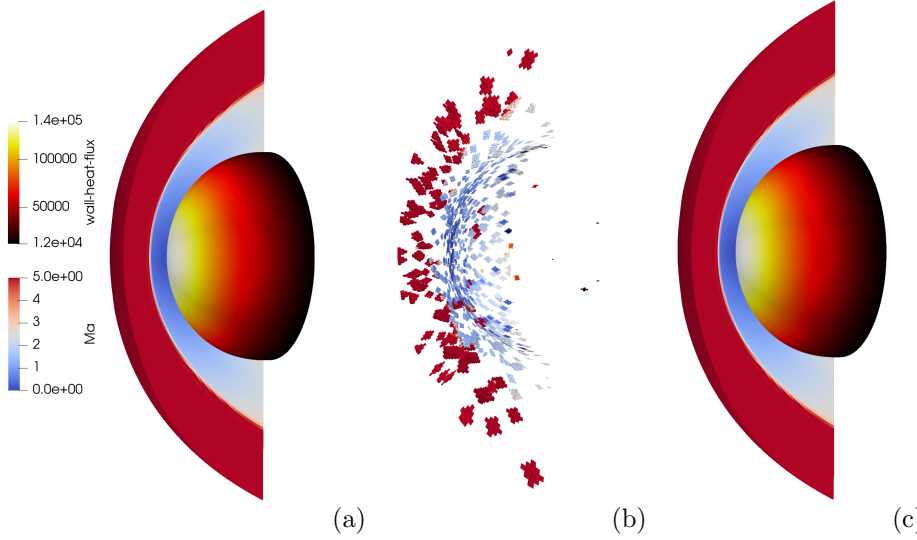


FIG. 3. Three-dimensional visualizations of the Blottner sphere problem at the final time step (i.e., steady state) displaying the flow color-coded by the Mach number (M) and the sphere surface color-coded by the local heat flux. Panel (a) shows the results from a full-order model simulation. Panels (b,c) show those obtained from the LSPG ROM with 8 POD modes and 1% sample mesh: in (b) we show the sample mesh only, and in (c) we plot the ROM-based solution reconstructed over the full mesh.

accurately reproduces the FOM results. Since this is a reproductive ROM, when we use the full set of POD modes, $p = 64$, one would expect to recover the FOM state committing an error that is close to machine zero. For this test case, this does not occur because, as anticipated before, the convergence criterion for both the FOM and ROM nonlinear solvers is not the absolute norm of the residual reaching machine zero, rather a reduction of its relative norm. Hence, this tolerance poses a limitation. We remark that a convergence criterion based on the relative residual norm reduction is typical for large-scale CFD problems, since obtaining machine zero is generally unfeasible.

Performance: Figure 4 summarizes performance results in terms of the computational cost reduction factor of the LSPG ROM with respect to the FOM, computed as the ratio between the FOM core-hours and ROM core-hours. The results are grouped by the sample mesh size. The computational savings for the hyper-reduced ROMs are substantial. The largest speed up ($> 100X$) is obtained with the 1% sample mesh and $p = 8$, while the smallest ($\sim 5X$) is obtained with the 10% sample mesh and $p = 64$. It is also interesting to note that the ROM *without* hyper-reduction yields a gain when using $p = 8$. As expected, if the reduced system is large enough and no hyper-reduction is used, the cost of the ROM is larger than the FOM, as seen for sm_{100} and $p \in 16, 32, 64$.

4.2. pressio4py vs. pressio native C++. In this section, we discuss the performance and overhead incurred when using **pressio4py** rather than **Pressio** directly from C++. We consider a reproductive scenario with an inviscid Burgers problem

	p	state error		heat-flux error		wall-shear error	
		ℓ^2 -norm	ℓ^∞ -norm	ℓ^2 -norm	ℓ^∞ -norm	ℓ^2 -norm	ℓ^∞ -norm
sm ₁	08	5.013e-04	5.621e-03	2.912e-03	3.581e-03	1.644e-03	3.586e-03
	16	8.354e-05	9.039e-04	1.838e-04	4.528e-04	1.796e-04	6.041e-04
	32	2.807e-05	1.850e-04	2.193e-04	3.115e-04	1.517e-04	3.369e-04
	64	1.617e-04	2.412e-03	7.174e-04	1.086e-03	4.218e-04	8.570e-04
sm ₂	08	4.396e-04	5.478e-03	1.594e-03	3.242e-03	1.055e-03	3.478e-03
	16	9.335e-05	9.974e-04	7.033e-04	1.105e-03	4.197e-04	1.040e-03
	32	1.114e-05	1.098e-04	9.334e-05	1.529e-04	4.903e-05	1.273e-04
	64	4.603e-06	5.229e-05	2.660e-05	4.312e-05	1.555e-05	4.300e-05
sm ₅	08	4.404e-04	5.210e-03	1.754e-03	2.824e-03	9.739e-04	2.741e-03
	16	1.356e-04	1.016e-03	1.196e-03	1.844e-03	7.411e-04	1.786e-03
	32	1.000e-05	1.076e-04	9.340e-05	1.461e-04	4.829e-05	1.177e-04
	64	1.564e-06	2.426e-05	8.238e-06	1.429e-05	4.649e-06	1.325e-05
sm ₁₀	08	5.318e-04	4.589e-03	2.066e-03	3.460e-03	1.184e-03	3.178e-03
	16	9.858e-05	9.816e-04	7.987e-04	1.228e-03	4.781e-04	1.159e-03
	32	7.368e-06	9.632e-05	6.368e-05	1.025e-04	3.205e-05	7.851e-05
	64	9.215e-07	1.520e-05	2.509e-06	4.087e-06	1.840e-06	4.707e-06
sm ₁₀₀	08	5.073e-04	4.563e-03	2.048e-03	2.865e-03	1.162e-03	2.546e-03
	16	8.075e-05	1.033e-03	6.144e-04	9.334e-04	3.705e-04	9.445e-04
	32	3.753e-06	1.036e-04	1.257e-05	2.557e-05	6.534e-06	2.187e-05
	64	9.849e-07	7.747e-06	4.059e-06	6.564e-06	3.121e-06	8.260e-06

TABLE 1

Relative norms of the errors for target observables between the ROM prediction and the full-order model results of the Blottner sphere problem. The metrics are computed at steady state.

written in the conservative form

$$\begin{aligned}
 (4.1) \quad & \frac{\partial u(x, t)}{\partial t} + \frac{1}{2} \frac{\partial(u^2(x, t))}{\partial x} = \alpha \exp(\beta x), \\
 & u(0, t) = \gamma, \forall t > 0, \\
 & u(x, 0) = 1, \forall x \in [0, 100],
 \end{aligned}$$

where u is the state variable, x represent the spatial variable, t is time, and α, β, γ are real-valued parameters chosen as $\alpha = \beta = 0.02$ and $\gamma = 5$. We use a finite-volume spatial discretization with N cell of uniform width and Godunov upwinding. The semi-discrete version of the problem above takes the form of Eq. (1.1). We explore full-order models of varying dimension $N = 2^k$, with $k \in \{10, 11, 12, 13, 14, 15\}$. Below, we purposefully limit our attention to performance and overhead, and omit a discussion of the accuracy of the ROM which, for the problem above, can be found in, e.g., [27].

We have developed two implementations of the full-order problem in (4.1), one in Python that meets the API shown in listing 2, and one in C++ using Eigen¹² data structures that meets the API shown in listing 1. The Python implementation uses NumPy and SciPy, and is optimized with Numba decorators to translate target loops—in the velocity and Jacobian calculation—to optimized machine code at run-

¹²<http://eigen.tuxfamily.org>

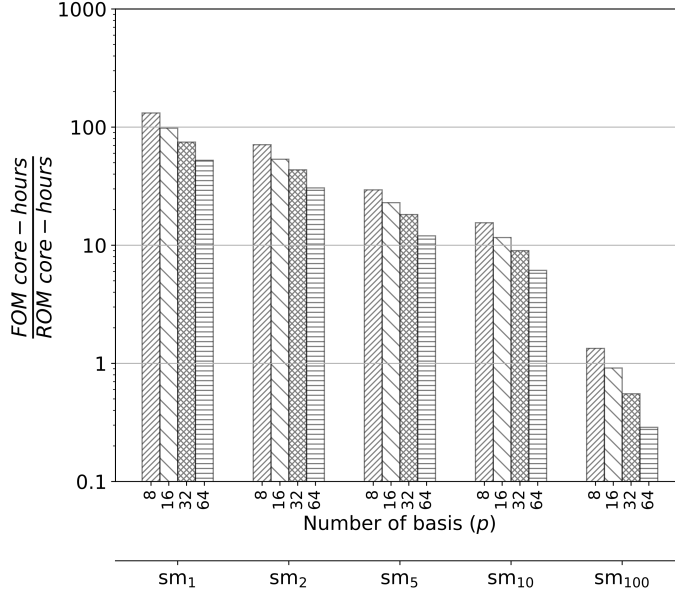


FIG. 4. Performance results for the Blottner sphere test case showing the core-hours reduction factor of the LSPG ROM with respect to the full order model. Each data point is obtained by computing the geometric mean of a set of three runs. The hyper-reduced ROM cases (identified by labels sm_1 , sm_2 , sm_5 and sm_{10}) are run on a single node, while the ROM without hyper-reduction (sm_{100}) uses 32 nodes to distribute the mesh.

time. We use OpenBLAS 0.3.7¹³ built with GCC 9.2.0 as a linear algebra backend for both NumPy/SciPy and Eigen ensuring that all computations involving dense operators call the same BLAS/LAPACK routines at the lowest level.

We focus on two reduction methods: Galerkin projection as in (2.6) using a 4th-order explicit Runge–Kutta time integrator and LSPG (2.9) with a backward Euler time stepper. For both Galerkin and LSPG, we consider ROMs of dimension $p \in \{32, 64, 128, 256\}$. In all cases, we use $\mathbf{A} = \mathbf{I}$ (the benefits of hyper-reduction are outside the scope of this section), use the initial condition $u(x, 0) = 1$ as reference state, and employ a linear trial subspace for projection. To compute the basis for Galerkin, we run the full-order model over the interval $t \in [0, 2.048]$ using a 4th-order Runge–Kutta scheme, collecting the snapshot matrix, subtracting the initial condition $u(x, 0) = 1$ from each snapshot and computing the POD. To compute the basis vectors for LSPG, we use the same procedure except that a backward Euler time scheme is used over a time interval $t \in [0, 0.512]$. The time interval chosen for LSPG is shorter than the one for Galerkin because LSPG is more expensive, and this setup allows us to have a reasonable turnaround time for both. In all cases, the resulting total number of steps can be exactly factorized by any of the selected reduced dimensions p , and we use a time step $\Delta t = 5 \times 10^{-4}$, ensuring stability for all simulations.

For LSPG, we solve the nonlinear least-squares problem at each time step using a Gauss–Newton solver implemented in **Pressio** that assembles and solves the normal equations. To solve the normal equations, we use the **getrf** direct LU-based solver from LAPACK. In Python, one can directly call **getrf** via the low-level LAPACK

¹³<https://www.openblas.net/>

functionalities in `scipy.linalg.lapack`. In Eigen, built with LAPACK support, `getrf` is the implementation underlying the LU decomposition of a dense matrix.

For LSPG, an important detail is the data structure type used for the spatial Jacobian arising from the semi-discrete formulation of the system in (4.1). In general, spatial Jacobian operators for problems involving local information (e.g., finite differences and finite volumes) are sparse by definition and, thus, typically represented as sparse matrices due to the smaller memory footprint. For the purposes of this analysis, one caveat is that using a sparse Jacobian implies using the native implementations in SciPy and Eigen, since we cannot rely on a common backend. For a dense Jacobian, instead, as anticipated before, we can rely on the same BLAS backend. To this end, we developed two versions of the spatial Jacobian for problem (4.1), one relying on a sparse and one on a dense matrix representation. This allows us to quantify the overhead of **pressio4py** with and without biases due to different implementations. For all dense operators, we use column-major ordering, yielding seamless compatibility with the native Fortran API of BLAS/LAPACK, while for the sparse Jacobian we use the Compressed Sparse Row (CSR) format.

Figure 5 shows the results obtained for Galerkin (a), and LSPG when using a sparse (b) and dense (c) matrix for the application’s spatial Jacobian. Each plot displays, in a semi-log scale, the time per iteration (in milliseconds) as a function of the mesh size, obtained with the native C++ in **Pressio** and **pressio4py** for selected values of the ROM size, p . Each data point is the geometric mean of a sample of 10 replica runs, and error bars are omitted because the statistical variability is negligible. All runs were completed as single-threaded processes on a dual socket machine, containing two 18-core Intel(R) Xeon(R) Gold 6154 CPU @ 3.00GHz and 125GB of memory.

The plots show that Galerkin has the smallest time cost per iteration, while LSPG based on a dense Jacobian has the largest time per iteration. Figure 5 (a) shows that for Galerkin, up to about $N = 4096$, the C++ version perform slightly better than the Python one. However, as the mesh size increases, the two codes exhibit nearly identical performance. As expected, panel (b) shows that for LSPG with a sparse spatial Jacobian, the differences between C++ and Python are more evident, revealing the bias due to the different implementation. Panel (c) shows that when LSPG is run with a dense spatial Jacobian, the differences between the two codes are nearly indistinguishable. This analysis demonstrates that the overhead incurred due to the Python layer of **pressio4py** is effectively negligible.

5. Conclusions. This article presented **Pressio**, an open-source project aimed at enabling leading-edge projection-based reduced order models (ROMs) for large-scale nonlinear dynamical systems. We discussed the algorithms currently supported and those planned for upcoming releases, including the support for both linear and nonlinear trial manifolds, and the applicability to reduce both spatial and temporal degrees of freedom for any system expressible as a parameterized set of ODEs.

We described the minimal API required by **Pressio**, which is a natural choice for dynamical systems. To give an glimpse of the software design choices behind **Pressio**, we highlighted the use and benefits of generic programming. We discussed how the core C++ implementation of **Pressio** is complemented with Python bindings to expose these functionalities to Python users with negligible overhead and no user-required binding code.

We presented our experience with a production-level aerodynamic code, highlighting the minimal additions to the native code needed to construct the sample mesh and

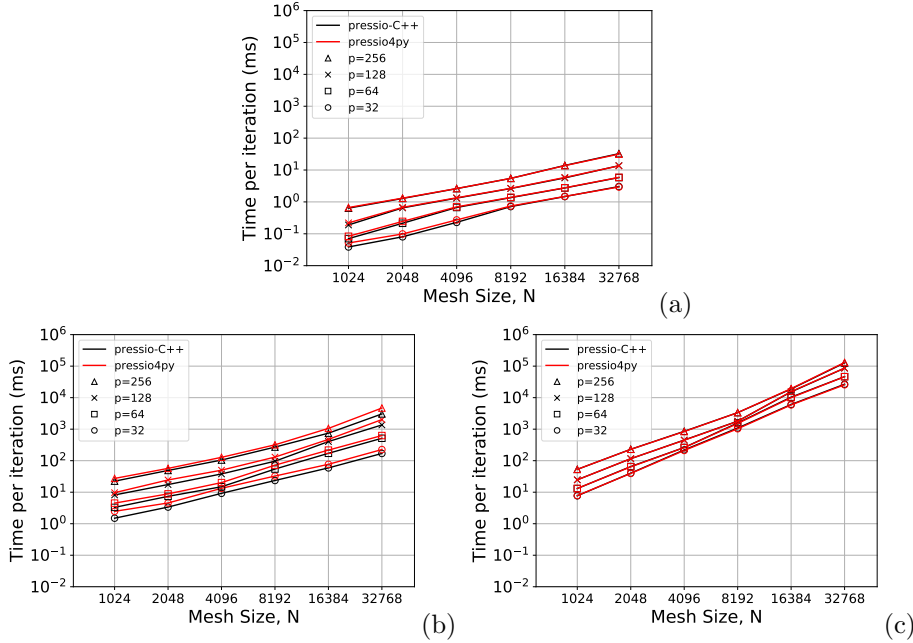


FIG. 5. Figure (a): time per iteration (milliseconds) as a function of the mesh size obtained for Galerkin ROM applied to problem (4.1) using the native C++ in **Pressio** and **pressio4py** for four different ROM sizes. Figure (b) shows the corresponding results obtained for LSPG using a sparse matrix for the spatial Jacobian in the Burgers implementation, while (c) shows those obtained using a dense Jacobian matrix.

apply the LSPG ROM. We showed the substantial computational performance gains obtainable using a sample mesh, and discussed how this should be evaluated in the context of a tradeoff between performance and accuracy. We then showed an example using the Python bindings library, **pressio4py**, which has a negligible overhead compared to using the core C++ **Pressio**.

We designed and implemented **Pressio** to be usable for both large-scale simulations, where performance is critical, and prototyping problems, where the focus is on assessing the accuracy of a new ROM technique. We are working on expanding the set of demonstration cases to explore advantages and disadvantages of ROMs for various types of problems, further improvements to performance, investigating various sample mesh techniques, and providing a default, automated functionality to run nonlinear ROMs based on convolutional autoencoders.

Acknowledgments. The authors thank Matthew Zahr for extremely helpful and insightful conversations that led to the inception of this project. The authors also thank Matthew David Smith, and Mark Hoemmen for helpful suggestions and feedback. This paper describes objective technical results and analysis. Any subjective views or opinions that might be expressed in the paper do not necessarily represent the views of the U.S. Department of Energy or the United States Government. Supported by the Laboratory Directed Research and Development program at Sandia National Laboratories, a multimission laboratory managed and operated by National Technology and Engineering Solutions of Sandia, LLC., a wholly owned subsidiary of Honeywell International, Inc., for the U.S. Department of Energy’s National Nuclear Security Administration under contract DE-NA-0003525. SAND2020-1279 J

and SAND2020-1445 J.

REFERENCES

- [1] C. BACH, L. SONG, T. ERHART, AND F. DUDDECK, *Stability conditions for the explicit integration of projection based nonlinear reduced-order and hyper reduced structural mechanics finite element models*, arXiv e-prints, (2018), arXiv:1806.11404, p. arXiv:1806.11404, <https://arxiv.org/abs/1806.11404>.
- [2] S. BALAY, S. ABHYANKAR, M. F. ADAMS, J. BROWN, P. BRUNE, K. BUSCHELMAN, L. DALCIN, A. DENER, V. ELJKHOUT, W. D. GROPP, D. KARPEYEV, D. KAUSHIK, M. G. KNEPLEY, D. A. MAY, L. C. MCINNES, R. T. MILLS, T. MUNSON, K. RUPP, P. SANAN, B. F. SMITH, S. ZAMPINI, H. ZHANG, AND H. ZHANG, *PETSc users manual*, Tech. Report ANL-95/11 - Revision 3.12, Argonne National Laboratory, 2019, <https://www.mcs.anl.gov/petsc>.
- [3] S. BALAY, W. D. GROPP, L. C. MCINNES, AND B. F. SMITH, *Efficient management of parallelism in object oriented numerical software libraries*, in Modern Software Tools in Scientific Computing, E. Arge, A. M. Bruaset, and H. P. Langtangen, eds., Birkhäuser Press, 1997, pp. 163–202.
- [4] M. BAUMANN, P. BENNER, AND J. HEILAND, *Space-time Galerkin POD with application in optimal control of semi-linear parabolic partial differential equations*, arXiv preprint arXiv:1611.04050, (2016).
- [5] B. A. BELSON, J. H. TU, AND C. W. ROWLEY, *Algorithm 945: Modred — A Parallelized Model Reduction Library*, ACM Trans. Math. Softw., 40 (2014), pp. 30:1–30:23, <https://doi.org/10.1145/2616912>.
- [6] P. BLONIGAN, K. CARLBERG, F. RIZZI, M. HOWARD, AND J. FIKE, *Model reduction for hypersonic aerodynamics via conservative LSPG projection and hyper-reduction*, in AIAA SCITECH Forum, vol. 1, Orlando, FL, 2020, AIAA.
- [7] F. G. BLOTTNER, *Accurate Navier-Stokes results for the hypersonic flow over a spherical nosetip*, Journal of Spacecraft and Rockets, 27 (1990), pp. 113–122, <https://doi.org/10.2514/3.26115>.
- [8] M. BRAND, *Incremental Singular Value Decomposition of Uncertain Data with Missing Values*, in Computer Vision — ECCV 2002, A. Heyden, G. Sparr, M. Nielsen, and P. Johansen, eds., Berlin, Heidelberg, 2002, Springer Berlin Heidelberg, pp. 707–720.
- [9] K. CARLBERG, M. BARONE, AND H. ANTIL, *Galerkin v. least-squares Petrov–Galerkin projection in nonlinear model reduction*, Journal of Computational Physics, 330 (2017), pp. 693 – 734, <https://doi.org/10.1016/j.jcp.2016.10.033>.
- [10] K. CARLBERG, C. BOU-MOSLEH, AND C. FARHAT, *Efficient non-linear model reduction via a least-squares Petrov–Galerkin projection and compressive tensor approximations*, International Journal for Numerical Methods in Engineering, 86 (2011), pp. 155–181, <https://doi.org/10.1002/nme.3050>.
- [11] K. CARLBERG, C. FARHAT, J. CORTIAL, AND D. AMSALLEM, *The GNAT method for nonlinear model reduction: Effective implementation and application to computational fluid dynamics and turbulent flows*, Journal of Computational Physics, 242 (2013), pp. 623 – 647, <https://doi.org/10.1016/j.jcp.2013.02.028>.
- [12] K. CARLBERG, R. TUMINARO, AND P. BOGGS, *Preserving Lagrangian structure in nonlinear model reduction with application to structural dynamics*, SIAM Journal on Scientific Computing, 37 (2015), pp. B153–B184.
- [13] K. T. CARLBERG, Y. CHOI, AND S. SARGSYAN, *Conservative model reduction for finite-volume models*, Journal of Computational Physics, 371 (2018), p. 280–314.
- [14] H. CARTER EDWARDS, C. R. TROTT, AND D. SUNDERLAND, *Kokkos*, J. Parallel Distrib. Comput., 74 (2014), pp. 3202–3216, <https://doi.org/10.1016/j.jpdc.2014.07.003>.
- [15] S. CHATURANTABUT, C. BEATTIE, AND S. GUGERCIN, *Structure-preserving model reduction for nonlinear port-hamiltonian systems*, SIAM Journal on Scientific Computing, 38 (2016), pp. B837–B865.
- [16] Y. CHOI AND K. CARLBERG, *Space–Time Least-Squares Petrov–Galerkin Projection for Non-linear Model Reduction*, SIAM Journal on Scientific Computing, 41 (2019), pp. A26–A58, <https://doi.org/10.1137/17M1120531>.
- [17] DAVERSIN, C., VEYS, S., TROPHIME, C., AND PRUD’HOMME, C., *A reduced basis framework: Application to large scale non-linear multi-physics problems*, ESAIM: Proc., 43 (2013), pp. 225–254, <https://doi.org/10.1051/proc/201343015>.
- [18] C. FARHAT, T. CHAPMAN, AND P. AVERY, *Structure-preserving, stability, and accuracy properties of the energy-conserving sampling and weighting method for the hyper reduction of*

- nonlinear finite element dynamic models*, International Journal for Numerical Methods in Engineering, 102 (2015), pp. 1077–1110.
- [19] C. GU AND J. ROYCHOWDHURY, *Model reduction via projection onto nonlinear manifolds, with applications to analog circuits and biochemical systems*, in 2008 IEEE/ACM International Conference on Computer-Aided Design, IEEE, 2008, pp. 85–92.
 - [20] J. S. HESTHAVEN, G. ROZZA, AND B. STAMM, *Certified Reduced Basis Methods for Parametrized Partial Differential Equations*, SpringerBriefs in Mathematics, Springer International Publishing, 2015.
 - [21] A. C. HINDMARSH, P. N. BROWN, K. E. GRANT, S. L. LEE, R. SERBAN, D. E. SHUMAKER, AND C. S. WOODWARD, *SUNDIALS: Suite of nonlinear and differential/algebraic equation solvers*, ACM Transactions on Mathematical Software (TOMS), 31 (2005), pp. 363–396.
 - [22] P. HOLMES, J. LUMLEY, AND G. BERKOOZ, *Turbulence, Coherent Structures, Dynamical Systems and Symmetry*, Cambridge University Press, 1996.
 - [23] M. HOWARD, A. BRADLEY, S. W. BOVA, J. OVERFELT, R. WAGNILD, D. DINZL, M. HOEMMEN, AND A. KLINVEX, *Towards Performance Portability in a Compressible CFD Code*, in 23rd AIAA Computational Fluid Dynamics Conference, vol. 1, Denver, CO, 2017, AIAA, <https://doi.org/10.2514/6.2017-4407>.
 - [24] W. JAKOB, J. RHINELANDER, AND D. MOLDOVAN, *pybind11 – Seamless operability between C++11 and Python*, 2017. <https://github.com/pybind/pybind11>.
 - [25] B. S. KIRK, J. W. PETERSON, R. H. STOIGNER, AND G. F. CAREY, *libMesh: A C++ Library for Parallel Adaptive Mesh Refinement/Coarsening Simulations*, Engineering with Computers, 22 (2006), pp. 237–254, <https://doi.org/10.1007/s00366-006-0049-3>.
 - [26] D. J. KNEZEVIC AND J. W. PETERSON, *A high-performance parallel implementation of the certified reduced basis method*, Computer Methods in Applied Mechanics and Engineering, 200 (2011), pp. 1455–1466, <https://doi.org/10.1016/j.cma.2010.12.026>.
 - [27] K. LEE AND K. T. CARLBERG, *Model reduction of dynamical systems on nonlinear manifolds using deep convolutional autoencoders*, Journal of Computational Physics, 404 (2020), p. 108973.
 - [28] R. W. MACCORMACK, *Carbuncle Computational Fluid Dynamics Problem for Blunt-Body Flows*, Journal of Aerospace Information Systems, 10 (2013), pp. 229–239, <https://doi.org/10.2514/1.53684>.
 - [29] D. S. MEDINA, A. ST-CYR, AND T. WARBURTON, *OCCA: A unified approach to multi-threading languages*, arXiv preprint arXiv:1403.0968, (2014).
 - [30] R. MILK, S. RAVE, AND F. SCHINDLER, *pyMOR – Generic Algorithms and Interfaces for Model Order Reduction*, SIAM Journal on Scientific Computing, 38 (2016), pp. S194–S216, <https://doi.org/10.1137/15M1026614>.
 - [31] D. R. MUSSER AND A. A. STEPANOV, *Generic programming*, in Proceedings of the International Symposium ISSAC’88 on Symbolic and Algebraic Computation, ISAAC ’88, London, UK, UK, 1989, Springer-Verlag, pp. 13–25, <http://dl.acm.org/citation.cfm?id=646361.690581>.
 - [32] E. J. PARISH AND K. T. CARLBERG, *Windowed least-squares model reduction for dynamical systems*, arXiv e-prints, (2019), arXiv:1910.11388, p. arXiv:1910.11388, <https://arxiv.org/abs/1910.11388>.
 - [33] V. PUZYREV, M. GHOMMEM, AND S. MEKA, *pyROM: A computational framework for reduced order modeling*, Journal of Computational Science, 30 (2019), pp. 157 – 173, <https://doi.org/10.1016/j.jocs.2018.12.004>.
 - [34] C. ROWLEY, *Model reduction for fluids, using balanced proper orthogonal decomposition*, Int. J. on Bifurcation and Chaos, 15 (2005), pp. 997–1013.
 - [35] P. J. SCHMID, *Dynamic mode decomposition of numerical and experimental data*, Journal of fluid mechanics, 656 (2010), pp. 5–28.
 - [36] K. URBAN AND A. T. PATERA, *A new error bound for reduced basis approximation of parabolic partial differential equations*, Comptes Rendus Mathématique, 350 (2012), pp. 203–207.
 - [37] K. M. WASHABAUGH, *Fast Fidelity for Better Design: A Scalable Model Order Reduction Framework for Steady Aerodynamic Design Applications*, PhD dissertation, Stanford University, Department of Aeronautics and Astronautics, Aug. 2016.
 - [38] K. WILLCOX AND J. PERAIRE, *Balanced model reduction via the proper orthogonal decomposition*, AIAA Journal, 40 (2002), pp. 2323–2330.
 - [39] M. YANO, *A space-time Petrov–Galerkin certified reduced basis method: Application to the boussinesq equations*, SIAM Journal on Scientific Computing, 36 (2014), pp. A232–A266.
 - [40] M. YANO, *Discontinuous Galerkin reduced basis empirical quadrature procedure for model reduction of parametrized nonlinear conservation laws*, Advances in Computational Mathematics, (2019), pp. 1–34.

SUPPLEMENTARY MATERIALS: PRESSIO: ENABLING PROJECTION-BASED MODEL REDUCTION FOR LARGE-SCALE NONLINEAR DYNAMICAL SYSTEMS *

FRANCESCO RIZZI[†], PATRICK J. BLONIGAN[‡], ERIC J. PARISH[‡], AND
KEVIN T. CARLBERG^{‡§}

SM1. Software design overview. In this section, we provide an overview of key software engineering aspects of **Pressio** aiming at (a) describing how we abstract mathematical concepts into classes; (b) providing a coarse-grained overview of the various components and their connections; and (c) explaining the design choices behind the API required by **Pressio**. To convey the main ideas clearly and concisely, we describe at a high level representative classes needed for a Galerkin ROM with an explicit time integration, deliberately omitting overly fine-grained details about classes, methods and syntax, which we believe would be more distracting than useful. We refer the reader interested in the full implementation details to the source code of **Pressio** and its documentation directly.

Figure [SM1](#) shows a (simplified) UML (Unified Modeling Language) class diagram of the main classes needed for a Galerkin ROM using an explicit time stepping scheme. For the sake of readability, wherever possible, we denote arguments and variables with the same notation used in § 2 of the paper. A similar schematic for LSPG can be found in [SM1.2](#).

To discuss the UML diagram in [SM1](#), we start from the `DefaultProblem` class. This class template represents the default Galerkin problem, namely Eq. 2.6 in the paper with $\mathbf{A} = \mathbf{I}$. It needs as template arguments a (tag) type `stepperTag`, and types for the ROM state, adapter class and decoder. `stepperTag` is used for tag dispatching, and can be chosen from a set of options, e.g., `ode::explicitmethods::Euler` or `ode::explicitmethods::BDF2`. The variadic nature of the class facilitates the user since the template arguments can be passed in arbitrary order. We use metaprogramming to expand the pack and detect the needed types according to specific conditions. For example, a type is detected as a valid adapter class type only if it satisfies the API discussed in listing 1 in the paper. Other conditions are used to detect the state and decoder types. If **Pressio** does not find admissible template arguments, a compile-time error is thrown. An object instantiated from the class template `DefaultProblem` is responsible for constructing a policy of type `DefaultVelocityPolicy`, a stepper object of type `ExplicitStepper`, and a reconstructor object of type `FomStateReconstructor`. The policy defines *how* the right-hand-side (velocity) of the Galerkin system is computed, the stepper defines how to advance the system over a single time step, and the reconstructor holds the information and data (i.e., the decoder) to map a given ROM state vector to a FOM model state. Once the Galerkin problem is instantiated, the contained stepper object can be used with one of the integrators available inside **Pressio/ode**.

*Submitted to the editors February 6th, 2020.

[†]NexGen Analytics, 30N Gould St. Ste 5912, Sheridan, WY, 82801, USA (francesco.rizzi@ng-analytics.com, fnrizzi@sandia.gov).

[‡]Department of Extreme-Scale Data Science and Analytics, Sandia National Laboratories, Livermore, CA, 94550, USA (pblonig@sandia.gov, ejparis@sandia.gov).

[§]Departments of Applied Mathematics and Mechanical Engineering, University of Washington, Seattle, WA 98195, USA

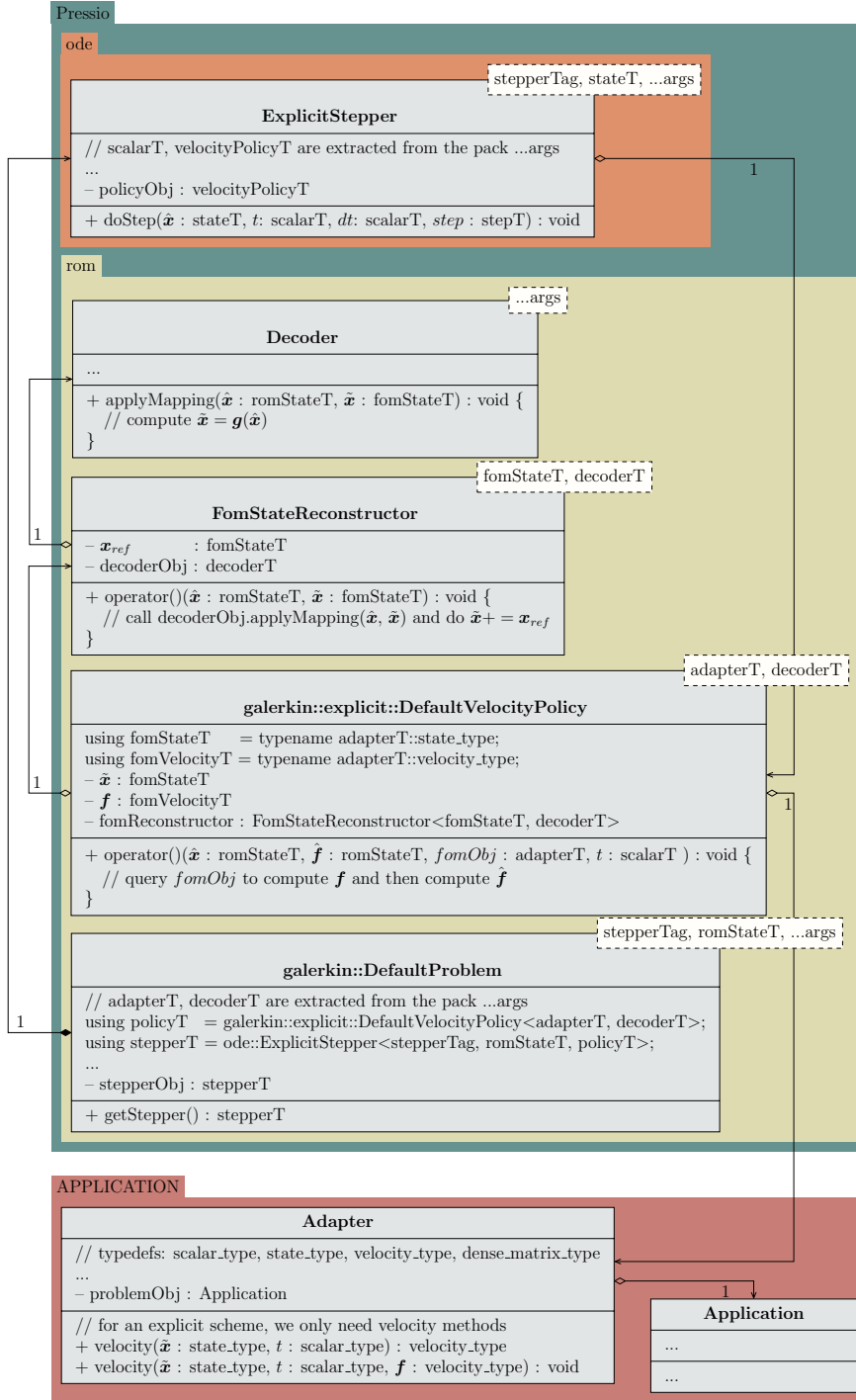


FIG. SM1. UML class diagram of the main classes defining a Galerkin ROM using an explicit time stepping scheme. For the sake of readability, we adopt a few simplifications: (a) wherever possible we use the same notation used in § 2 in the paper; (b) we omit base classes; (c) as non-standard extensions to the UML language, we use angle brackets $\langle \rangle$ to represent templates, and the C++ keyword `using` to represent type aliases in classes, respectively. These minimal simplifications allow us to make the diagram substantially more readable and to highlight the interdependencies in a clearer way.

The UML diagram highlights that the application *only* interacts with the policy class. The policy object, in fact, calls the `velocity` method inside the adapter, which in turn holds all the information about the FOM problem. Minimizing the number of direct connections between the application and **Pressio** yields a much leaner structure less prone to errors. The policy-based design seems a suitable choice allowing us to create new problems by only operating at a low level while keeping the interaction between the various components and the workflow intact. This is in fact how we support variations of the basic Galerkin: different policy (and problem) classes can be implemented encapsulating different ways to compute the right-hand-side shown in the formulations in Eq. 2.6.

SM1.1. Example main file for Galerkin ROM. The UML diagram description above enabled us to reason about the global structure and interdependencies between the classes. This section presents a sample main file and a description of how to create and run a Galerkin ROM. Listing 1 shows the skeleton of a C++ main file to instantiate and run a default Galerkin ROM with forward Euler. We highlight the following parts. On line 10, the user creates an object of the adapter class (which, underneath, is expected to create a full problem of the target application). A decoder object is created on lines 15–17. In this case, the listing shows a linear decoder, which is defined by its Jacobian. On line 20, a reference state for the full order model is defined, and on line 23 the ROM state is defined. The actual Galerkin problem is instantiated on lines 26–30. The reader can cross-reference this class and its template arguments with the UML diagram in Figure SM1. Finally, after the problem is created, the actual time integration is run on line 34. For simplicity, we show here how to integrate for a target number of steps, but other integration options are available. **Pressio**, in fact, is implemented such that the concept of a stepper (whose responsibility is to only perform a single step) is separated from how the stepper is used to advance in time. This allows us to easily support different integrators (e.g. supporting variable time steps, running until a fixed time is reached, or until a user-provided condition is met).

SM1.2. Software Design for LSPG. Figure SM2 shows a simplified UML diagram of the main classes composing an unsteady LSPG problem. The `LSPGProblem` class is responsible for constructing an object of the policy class `LSPGResidualPolicy`, one of the policy class `LSPGJacobianPolicy`, one of the stepper class `ImplicitStepper`, and one of the class `FomStateReconstructor`. In this case, due to the implicit time integration, we need two policies, one for the time-discrete residual and one for the time discrete Jacobian. The stepper defines how to advance the system over a single time step, and the reconstructor holds the information and data (i.e. the decoder) to map a given ROM state vector to a full-order model state. Once the LSPG problem is created, the associated stepper object is used to advance the ROM solution in time. To this end, given the implicit nature of the stepper, a solver object is needed as an argument to the `doStep` to solve the nonlinear system at a given time step. For LSPG, the solver can be instantiated from one of the least-squares solver classes inside the **Pressio/solvers** currently supporting various types of Gauss-Newton nonlinear solvers, e.g. using the normal equations or QR factorization with an optional line search. Alternatively, the user can provide a custom solver object. At compile-time, **Pressio** checks that the solver type is admissible by verifying that it satisfies a specific API, e.g. having a public method `solve` accepting specific arguments.

The workflow is thus as follows: the time integrator (instantiated in the main, not shown here) chosen by the user calls `stepperObj.doStep`, which triggers the solver

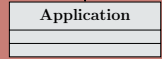
LISTING 1

Sample C++ main to create and run (explicit) Galerkin using Pressio.

```

1 int main(int argc, char *argv[]){
2     using adapterT          = /*adapter class type*/;
3     using scalarT           = typename adapterT::scalar_t;
4     using fomStateT         = typename adapterT::state_t;
5     using decoderJacT       = typename adapterT::dmatrix_t;
6     using romStateT         = /*ROM state type*/;
7     using namespace pressio;
8
9     // create app or adapter object
10    adapterT fomObj(argc, argv, /*other args needed*/);
11
12    const std::size_t romSize = /*set the Rom size */;
13
14    // create the decoder, e.g. linear decoder
15    decoderJacT phi = /*load/compute the decoder's Jacobian*/;
16    using decoderT = rom::LinearDecoder<decoderJacT>;
17    decoderT decoderObj(phi);
18
19    // set the FOM reference state
20    fomStateT xRef = /*load/compute the fom reference state*/;
21
22    // define ROM state
23    romStateT romState(romSize);
24
25    // create the Galerkin problem
26    using stepperTag = ode::explicitmethods::Euler;
27    using rom::galerkin::DefaultProblem;
28    using galerkinT = DefaultProblem<stepperTag, romStateT,
29                                   adapterT, decoderT>;
30    galerkinT galerkinProb(fomObj, xRef, decoderObj, romState);
31
32    // advance in time (t0, dt, Nsteps must be defined somewhere)
33    // or one can use a different integrator
34    ode::integrateNSteps(galerkinProb, romState, t0, dt, Nsteps);
35
36    // map the final ROM state to the corresponding fom
37    auto xFomFinal = galerkinProblem.fomReconstructor()(romState);
38
39    return 0;
40 }
```

via `solver.solve`, which in turn triggers a callback to `stepperObj.residual` and `stepperObj.jacobian` to compute the time-discrete quantities. The `residual` and `jacobian` methods in the `ImplicitStepper` do not hold any implementation details, because they simply call the `compute` method of the corresponding policy objects. Similarly to the Galerkin problem discussed before, the classes for LSPG are designed such that only the policies hold references to and interact with the application. This policy-based design allows us to create various LSPG problems by only changing the policies, without altering the overall workflow.



notation and simplifications as in Figure SM1.

SM2. Repositories and Versions. The project and its components are accessible at:

- Project url: <https://github.com/Pressio>
- C++ source code: <https://github.com/Pressio/pressio>
- **pressio4py** source code: <https://github.com/Pressio/pressio4py>

SM2.1. Code version used for § 4.1. The version of **Pressio** used to generate the results in § 4.1 for the large-scale hypersonic flow can be easily obtained since we used a Git **tag** to mark the commit in our development. The procedure is as follows:

1. Clone the core C++ **Pressio** repository:

```
git clone https://github.com/Pressio/pressio.git
```
2. Checkout the version used by doing:

```
git checkout siscBlottnerSphere
```

SM2.2. Code versions used for § 4.2. The version of **Pressio** and **pressio4py** used to generate the results in § 4.2 can be obtained in a similar way as follows:

1. Clone the core C++ **Pressio** repository:

```
git clone https://github.com/Pressio/pressio.git
```

```
git checkout siscBurgers1d
```
2. Clone **pressio4py**:

```
git clone https://github.com/Pressio/pressio4py.git
```

```
git checkout siscBurgers1d
```
3. Clone the code for Burgers1d:

```
git clone https://github.com/Pressio/pressio-sisc-burgers1d.git
```